Doctoral Thesis

The physiological basis for color vision in the Eastern Pale Clouded yellow butterfly, *Colias erate*

Yuri Ogawa

The Graduate University for Advanced Studies [SOKENDAI]
Department of Evolutionary Studies of Biosystems

2013

Acknowledgements

I would like to thank Professor Kentaro Arikawa of the Graduate University for Advanced Studies (SOKENDAI), for his guidance, valuable advise, helpful criticism, ceaseless encouragement and critical reading of this thesis. I am also grateful to Professor Doekele Stavenga (University of Groningen, Netherlands) for valuable advise, encouragement and useful discussions.

I wish to thank Assistant Professors Michiyo Kinoshita and Atsuko Matsushita (SOKENDAI) and Dr. Hiroko Awata (SOKENDAI) for tutelage of experiment and useful discussions. I wish to thank Drs Primož Pirih and Bodo Wilts for the care while I was staying at University of Groningen.

I wish to thank Dr Atsushi Nagayama who provided help in acquiring *Catopsilia pomona*, Drs Hisashi Otsuki and Hisaharu Koshitaka for extensive discussion, and Dr Finlay Stewart for editing the English. I give many thanks to all members of the laboratory for all they have done for me.

I thank JSPS (Japan Society for the Promotion of Science) graduate student fellowship, DC2 for the financial support.

Lastly, I want to express my deepest gratitude to my entire family and all of my friends who always have supported and encouraged me.

January 2013

Contents

General Introduction

Color vision is one of the most important visual functions and shared by a vast variety of animals including insects. Although many studies have been carried out in both vertebrates and invertebrates, the evolutionary and neuronal mechanisms underlying color vision are complex enough and still presenting us a number of interesting questions. Since the first behavioural demonstration by von Frisch of the ability of bees to discriminate colors, a number of studies have dealt with spectral sensitivity in insects (Frisch 1914; Menzel 1979; Kelber et al. 2003). As represented by honeybee, the majority of insects have a color vision system based on three types of photoreceptors, each peaking at the ultraviolet (UV), blue (B) and green (G) wavelength region: their color vision is trichromatic based on these photoreceptors (Menzel and Backhaus 1989). Compared to the majority of insects, the eyes of butterflies are much more complex, because they can be furnished with at least six spectral classes of receptors, as was shown for the Japanese yellow swallowtail butterfly, *Papilio xuthus* (Arikawa et al. 1987; Arikawa 2003). Butterflies have indeed highly sophisticated spectral discrimination systems, mediating for example detecting rewarding flowers, discriminating potential mates, and laying eggs on high quality leaves to safely feed their offspring immediately after hatch (Kelber 1999a; Kelber and Pfaff 1999; Kinoshita et al. 1999; Kinoshita and Arikawa 2000; Zaccardi et al. 2006; Kinoshita et al. 2008; Koshitaka et al. 2008).

How do butterflies produce photoreceptors of various spectral sensitivities? This is the question that I have focused throughout the study. The compound eyes of many butterflies share basic cellular organization, which are composed of several thousands of ommatidia, each containing nine photoreceptor cells, R1-9 (Yagi and Koyama 1963; Gordon 1977; Kolb 1978). These cells bear photoreceptive microvilli, together forming a three-tiered fused rhabdom in most of butterflies. The distal tier is composed of the microvilli of R1-4, whereas the proximal tier is made up of the microvilli of R5-8. The basal photoreceptor R9 bears microvilli immediately distal to the basement membrane. In some butterflies, photoreceptors R5-8 contain red perirhabdomal pigment whose arrangement designates three types of ommatidia. Although the basic structure of the eye is shared by many butterfly species, detailed anatomical and physiological studies have revealed extensive inter-specific variations. How such variations are evolved? What sort of biological meaning exist behind the variations? In order to establish broader views on the evolutional mechanisms of color vision system, comparative studies on carefully selected butterfly species are particularly useful.

The family Pieridae contains four subfamilies, Pierinae, Coliadinae, Dismorphiinae and

Pseudopontiinae (Braby 2006). The spectral organization of the small white butterfly, *Pieris rapae*, a member of the Pierinae, has been described in detail (Qiu et al. 2002; Qiu and Arikawa 2003a, b; Arikawa et al. 2005). For a subset of the comparative study, I thus selected the Eastern Pale Clouded yellow butterfly, *Colias erate*, a member of the Coliadinae. The compound eye of *Colias erate* is composed of about 6500 ommatidia, each containing nine photoreceptors (R1-9), forming a tiered rhabdom, surrounded by four clusters of reddish pigment granules in transverse section. The ommatidia are divided into three types (I-III) due to the arrangement of perirhabdormal pigment clusters and expression pattern of four opsin mRNAs, which had already been identified: they are one short (CeUV), two middle (CeV1, CeV2) and one long wavelength (CeL) -absorbing types (Awata et al. 2009). The spectral sensitivities of photoreceptors have also been recorded and divided into 9 classes by electrophysiological method (Pirih et al. 2010). However, the distribution of these spectral photoreceptors in the eye has remained unknown.

I thus decided to reveal the physiological basis of color vision system in *Colias erate*. In chapter 1 of this thesis, I demonstrate that *Colias* has regionalized and sexually different eyeshine (reflection from the tracheal tapetum) and spectral sensitivity of the entire eye determined by electroretinographic method. In chapter 2, I describe the spectral sensitivity of distal photoreceptors in three types of ommatidia in the male and female. In the course of the physiological study, I identified a novel opsin mRNA, which is coexpressed with CeV1 and CeV2 in a single photoreceptor. In chapter 3, I present another set of results of electrophysiology and histology revealing the sexual dimorphism in long wavelength receptors localized in the proximal tier of the ommatidia. I then compare the possible color discrimination properties of *Colias erate* with that of *Pieris rapae*. Finally, I discuss the physiological mechanism underlying the variety of spectral receptors in insects with the specific attention to its evolution.

Chapter 1

Regionalization and sexually dimorphism in compound eye of the Eastern Pale Clouded yellow butterfly, *Colias erate*

Abstract

The compound eye of *Colias erate* is composed of about 6500 ommatidia, each containing nine photoreceptors (R1-9), forming a tiered rhabdom, surrounded by four reddish pigments. The ommatidia are divided into three types (I-III) due to the arrangement of perirhabdormal pigment spots and expression pattern of four opsin mRNAs. I demonstrated here *Colias* eyes shine with epi-illumination lights, which are longer than 620 nm in both sexes. All ommatidia have identical reflectance spectrum in dorsal region of the eye in both sexes. Though type I ommatidia reflect 660 nm and type II and III ommatidia reflect 730 nm in male, female type II ommatidia reflect throughout 620 to 730 nm but type I and III reflect 660 nm 730 nm as in male, respectively. Remarkable sexual difference of eyeshine spectrum in type II ommatidia results from female specific orange pigment. Regionalization was also found by electroretinography. Dorsal region of retina relatively sensitivities below 420 nm range, whereas ventral region sensitivities to 420 nm to 550 nm due to ommatidial distribution bias.

Introduction

Butterfly eye is the assembly of thousands of ommatidia. When observed with an epi-illumination microscope, the eyes of most butterflies exhibit a colorful eyeshine, due to the presence of a tapetum reflector at the bottom of the rhabdom with the exception of all papilionids and some pierids (Bernard and Miller 1970; Stavenga et al. 2001; Takemura et al. 2007). The tapetum is formed by tracheae fold into a stack of layers, alternately consisting of air and cytoplasm, thus creating an interference reflection mirror. The tapetum reflects light that has escaped absorption while travelling through the rhabdom. Part of the reflected light travels through the rhabdom again and leaves the eye, which is then visible as the eyeshine. The eyeshine spectrum depends mainly on the spectral filtering by the pigment clusters surrounding the rhabdoms and characteristics of the tapetum, and thus the different colors of eyeshine indicate that ommatidia have different spectral properties.

Under white light epi-ilumination, the eye of the Eastern Pale Clouded yellow butterfly, *Colias erate*, shines bright red color only in the dorsal one third. Although remaining ventral two thirds of the eye seems totally dark for humans, in fact the majority of ommatidia have a peak reflectance at wavelengths longer than 700 nm, which are outside of our visible light range (Arikawa et al. 2009; Awata et al. 2009). The eyeshine spectrum peaking at long wavelengths is attributed to the absorption of red perirhabdomal pigment in the ommatidia. The bright red and infrared eyeshines are related to reduced and normal amount of perirhabdomal pigments in the dorsal and ventral region of the eye, respectively. Moreover, though all ommatidia contain identical red perirhabdomal pigment in males, I found that some ommatidia have orange perirhabdomal pigment in the ventral eye of female *Colias*. The orange pigment might result in differently colored eyeshine and sexually dimorphic spectral property of photoreceptors. I therefore closely investigated the eyeshine of *Colias* eyes and the spectral sensitivity of entire eye by electroretinography.

In the eye of female *Colias* tapetal reflection do exist on both dorsal and ventral region as in male. The eyeshine of dorsal region in female is similar to it in male, but some ommatidia in ventral eye region reflect 620 nm light only in female. Based on subsequent anatomical work, I found the ommatidia reflecting 620 nm contain orange pigment exclusively. The electroretinogram (ERG) of dorsal region of retina was remarkably different from in ventral retina at shorter wavelength in both sexes. However, the difference of spectral response between sexes was not significantly detected in both dorsal and ventral region.

Materials and Methods

Animal

Adults of the Eastern Pale Clouded yellow butterfly, *Colias erate* Esper, were obtained from a laboratory culture derived from eggs laid by females captured around the Sokendai-Hayama campus, Kanagawa, Japan. Hatched larvae were reared under natural light condition on fresh clover leaves.

Anatomy

I observed and photographed an intact eye using a modified telemicroscopic optical assembly (Stavenga 2002) equipped with an objective lens with a large numerical aperture and long working distance (Olympus LUCplanFLN20X, NA 0.45, WD 6.4-7.6 mm) under monochromatic lights (620 nm, 640 nm, 660 nm and 730 nm). To correlate the ommatidial tapetum reflection with pigmentation, I subsequently fixed the observed eye in 4 % paraformaldehyde in 0.1 mol sodium cacodylate buffer, pH 7.4, at room temperature for 30 min, embedded in Quetol 812 (Nisshin EM, Tokyo, Japan) and made semi-thin transverse sections. I observed the sections with a microscope (Olympus, BX50) to identify the ommatidial types by their pigmentation pattern under normal transmission light.

Imaging microspectrophotometry

For imaging microspectrophotometry (IMSP), I positioned an intact butterfly under the telemicroscope optical setup equipped with a Leitz LM32 NA 0.60 objective lens (Stavenga 2002). The spectra of ommatidial reflections were recorded in five spectral runs from 550 nm to 850 nm in 5 nm steps. The five runs were as follows: two reflection runs (up and down the spectrum), a calibration run with a MgO-coated surface on the stage instead of a butterfly, and their two respective background measurements, which served to correct for lens reflections. The time interval between the monochromatic flashes, 5 s, was sufficiently long to avoid light adaptation.

Electroretinogram

To determine the spectral sensitivity of the eye as a whole, I recorded electroretinogram (ERG). Monochromatic stimuli were provided by a 500 W Xenon arc lamp and through a series of narrow-band interference filters ranging from 300 to 740 nm. The light beam was focused on the tip of an optical fiber whose other end was attached to a device in a Faraday cage. The quantum flux of each monochromatic stimulus was measured using a radiometer (Model-470D, Sanso, Tokyo, Japan) and adjusted to a standard number of photons using an optical wedge. A butterfly whose wings and

legs were removed was fixed on a plastic stage with its dorsal or ventral side up and then mounted in the front of the exit pupil of the optical fiber. To record the ERG of the dorsal (ventral) region, I covered the ventral (dorsal) half of the eye with black paint. A chlorinated silver wire of Ø100 μm inserted into the head served as the indifferent electrode. Another Ø100 μm chlorinated silver wire was inserted into the retina through a hole made in the cornea. ERGs were recorded through a preamplifier (MEZ-7200; Nihon Kohden, Tokyo, Japan) connected to a computer via an AD converter (MP-150, BIOPAC Systems, USA). After two minutes dark adaptation, the spectral response was measured by a series of monochromatic flashes of duration 500 ms, spaced 25 s apart. The response-stimulus intensity (V-log I) function was recorded over a 4 log unit intensity range at the photoreceptor's peak wavelength. The V-log I data were fitted to the Naka-Rushton function, $V/V_{max} = I^n/(I^n + K^n)$, where I is the stimulus intensity, V is the response amplitude, V_{max} is the maximum response amplitude, K is the stimulus intensity eliciting 50 % of V_{max}, and n is the exponent. The data were further processed only when V_{max} exceeded 5 mV.

Results

Regionalization and sexual difference of eye shine

The eye of *Coliae erate* consists of dorsal and ventral part due to the difference in ommatidial property. To investigate the regionalization of the eye, I first observed the eyesine of both male and female *Colias* under monochromatic epi-illumination of 620, 640, 660 and 730 nm (Fig. 1-1). Dorsal part of the eye reflects wide range of wavelength from 620 nm to 660 nm in both sexes (Fig. 1-1a-c, e-g). The taperal reflection of the ventral region of males is divided into two, 660 nm (Fig. 1-1c) and 730 nm (Fig. 1-1d), as reported previously (Arikawa et al. 2009). Although the ventral ommatidia do not reflect 620 nm and 640 nm in the male, some ommatidia reflect all the tested wavelengths in the female (Fig. 1-1e-h).

Correlation of ommatidial type and taperal reflection in the female

The three types of ommatidia, I-III, are distinguishable by their characteristic patterns of perirhabdomal pigmentation. The ommatidial type and tapetal reflection are correlated in males (Arikawa et al. 2009), but not in females. I here tried to correlate the ommatidial type and tapetal reflection in females. I photographed and sectioned the photographed eye region for light microscopy. Type I and III ommatidia in females reflect 660 nm and 730 nm, respectively, as in males. However, type II ommatidia with square pigmentation reflect 620, 640, 660 and 730 nm (Fig. 1-2a-c). In female eyes the perirhabdomal pigments of type I and III ommatidia have the same red color as the pigment clusters of males, but in ommatidial type II the pigment is orange (Fig. 1-2d).

Imaging Microspectrophotometry of the tapetal reflection

I observed the tapetal reflection of the eye of *C. erate* using a telemicroscopic optical set up (Stavenga 2002). To measure the reflectance spectra of tapetum by the IMSP method, I illuminated the eye with a series of monochromatic lights produced by a monochromator. I analyzed the reflectance spectra of about 1100 and 900 ommatidia in the eye of male and female *Colias*, respectively. I could then correlate the spectra with ommatidial types according to the histological results. As described before (Arikawa et al. 2009), the reflectance spectra of the male eye were classified into three distinct types, dorsal (peak reflectance at 670 nm), ventral type I (680 nm) and ventral type II and III (740 nm) (Fig. 1-3a). In contrast, reflectance spectra of female ommatidia were divided into four; the dorsal (660 nm), ventral type I (670 nm), ventral type II (700 nm with broad 100 nm half-width) and ventral type III (730 nm) (Fig. 1-3b).

Electroretinogram

To investigate the regionalization of the compound eye physiologically, I measured the spectral sensitivity using the electroretinographic (ERG) method in both dorsal and ventral region of the eye (Fig. 1-4). I found that the sensitivity of ventral region is higher than that of dorsal region in the range from 420 nm to 560 nm in both sexes (Fig. 1-4). In addition to the dorso-ventral specialization, I found possible sexual dimorphism around 600 nm; in the ventral region, females seem to have higher sensitivity, while in the dorsal region, males seem to have higher sensitivity (Fig. 1-4).

Discussion

Eyeshine and tapetum

The eyeshine of butterflies is light reflected from the tapetum at the bottom of the rhabdom. The colored eyeshine therefore results form the optical system consisting of the spectrally selective reflecting tapetum and the rhabdom, which contains visual pigments and adjacent screening pigment acting as spectral filter (Ribi 1979; Stavenga 1979, 1989). The tapeta of the eyes of *Colias erate* reflect lights whose wavelength are longer than 620 nm in both sexes due to four reddish pigments surrounding the rhabdom in each ommatidium (Fig. 1-1). Most ommatidia in the dorsal region reflect 620 nm to 660 nm and their reflectance spectra are identical in both sexes, because all ommatidia share pale perirhabdomal pigment (Arikawa et al. 2009) (Fig. 1-3). On the other hand, a variety of eyeshine was found in the ventral region (Fig. 1-1). Among three ommatidial types, it has been already found that 660 nm-reflecting ommatidia are type I (trapezoidal pigment), while 730 nm-reflecting ommatidia are type II (square) and type III (rectangular) in males (see Arikawa et al., 2009 Fig. 3).

Based on these results, I classify the IMSP-measured reflectance spectra. The tapetum reflectance spectra of the male type I, II and III ommatidia rise up at about 620 nm (Fig. 1-3a). This property at the short wavelength side is determined by the transmittance spectrum of perirabdomal pigment. Therefore, all ommatidia in the ventral region of male eyes contain identical perirhabdomal pigment absorbing light whose wavelength is shorter than 620 nm. The higher reflectance value in type I is probably due to the trapezoidal arrangement of pigment around larger rhabdom (type I), which has lower filtering effect compared to the square and rectangular arrangements (type II and III). In contrast, the longer wavelength side of eyeshine spectrum is attribute to interference characteristics of tapetum. Both type II and III therefore possess identical tapetum at the end of rhabdom.

Situation is slightly different in females. In females, the pigment is orange in type II ommatidia while pigments in type I and III are red, which is identical to males (Fig. 1-2d). The orange pigment contributes to the broad-band eyeshine spectrum reflecting throughout 620 nm to 730 nm due to the absorption below 570 nm (Fig. 1-3b). This indicates that orange pigment is not pale version of the red pigment but consists of different substance from the red pigment (see Chapter 3).

In the small white butterfly, *Pieris rapae,* two classes of ommatidia are identified based on the eyeshine: 635 nm- and 670 nm-reflecting ommatidia respectively correspond to the

ommatidia with pale and deep red pigments located in the photoreceptor cell body adjacent to the rhabdoms (Qiu and Arikawa 2003b). In *Pieris rapae,* photoreceptors in the ommatidia with pale-red pigment have a spectral sensitivity peaking at 620 nm (red receptor, R) and those in ommatidia with deep-red pigment have sensitivity peaking at 640 nm (deep-red receptor, dR) (Qiu and Arikawa 2003b). Here I discovered three classes of tapetal reflection in female *Colias erate*. This might result in more variety of red receptors in females. Moreover, the some ommatidia of *Colias* have eyeshine peaking at 730 nm, almost in the infrared region, suggesting that the photoreceptors in these ommatidia may have a spectral sensitivity peaking at even longer wavelengths than those of *Pieris* (see Chapter 3).

Eye regionalization

To investigate the function of the regionalization and sexual dimorphism in the *Colias* eyes, I measured spectral sensitivities of the dorsal and the ventral regions separately by the ERG method. The ERG experiment, in which I insert thick electrode in the extracellular space in the retina, is suitable for analysing the eye sensitivity as a whole, but not suitable for acquiring information about single photoreceptors. Although remarkably sexual difference of ERG was not found, ventral region have slightly higher sensitivity around 600 nm in female. This might be related to variety of eyeshine suggesting the existence of red receptors in female (Fig. 1-4).

I detected a clear dorso-ventral specialization in ERG-determined spectral sensitivity. The dorsal region is more sensitive in the wavelength range from 420 nm to 560 nm in both sexes (Fig. 1-4). This regionalization is probably related to the distribution pattern of three ommatidial types. *Colias* ommatidia are divided into three types not only by arrangement of perirhabdomal pigment as described above, but also by the expression pattern of four opsin mRNAs in nine photoreceptor cells (R1-9). Four opsin mRNAs, one short (CeUV), two middle (CeV1, CeV2) and one long wavelength (CeL)-absorbing types, have been identified and localized in the eye of *Colias erate* (Awata et al. 2009). As the basic design of butterfly eyes, *Colias* has the short (S) and the middle (M) opsins in R1 and R2 in three fixed combinations, S-M, M-M and S-S, and the distribution pattern of S and M opsins corresponds to three ommatidial types, which is briefly as follows. In type I, R1 and R2 respectively expresses an S and M opsin or *vise versa*. In type II, both R1 and R2 express M opsin, and in type III both express S opsin (Wakakuwa et al. 2006). Although the same numbers of type I ommatidia exist in both dorsal and ventral regions, the occupancy ratio of type II ommatidia in the dorsal region is low, while type III ommatidia exist more in the dorsal region. The richness of type III ommatidia (S-S) implies the higher sensitivity (in a relative term) at

shorter wavelengths in the dorsal region. On the other hand, higher relative sensitivity of the ventral region in the middle wavelength region might be due to the type II ommatidia (M-M).

A sign of sexual dimorphism was also detected around 600 nm. This is probably related to the orange pigmentation of type II ommatidia in females. In addition to the ventral and dorsal regions, insect eyes are furnished with a specialized eye region for detecting sky polarization in the dorsal rim area (Kolb 1986; Horvath and Varju 2004; Labhart et al. 2009). I could not record ERG from the dorsal rim area in the present study, so the physiological properties of this specialized region remains for future study.

Figures

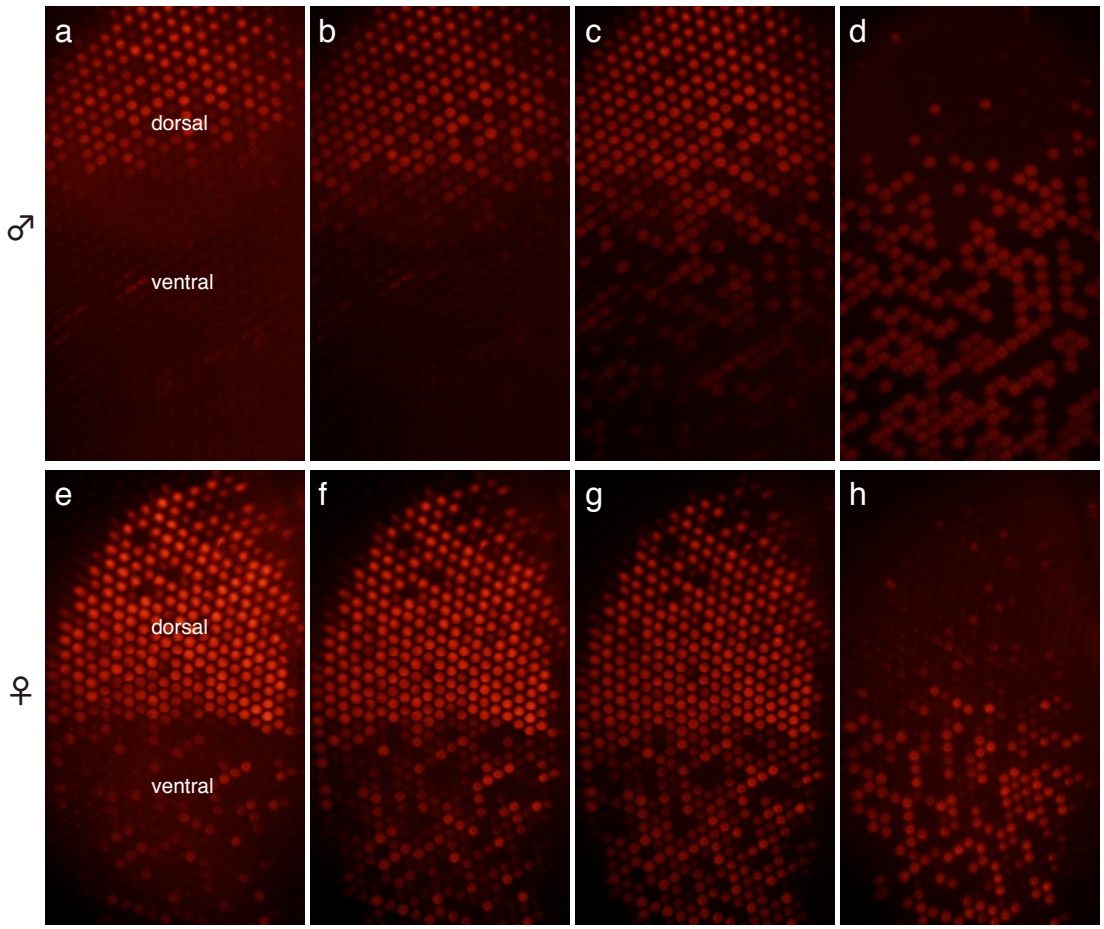

Fig. 1-1. Tapetal reflection of *Colias erate* male (**a**-**d**) and female (**e**-**h**) eyes under 620 nm (**a**, **e**), 640 nm (**b**, **f**), 660 nm (**c**, **g**) and 730 nm (**d**, **h**) illumination.

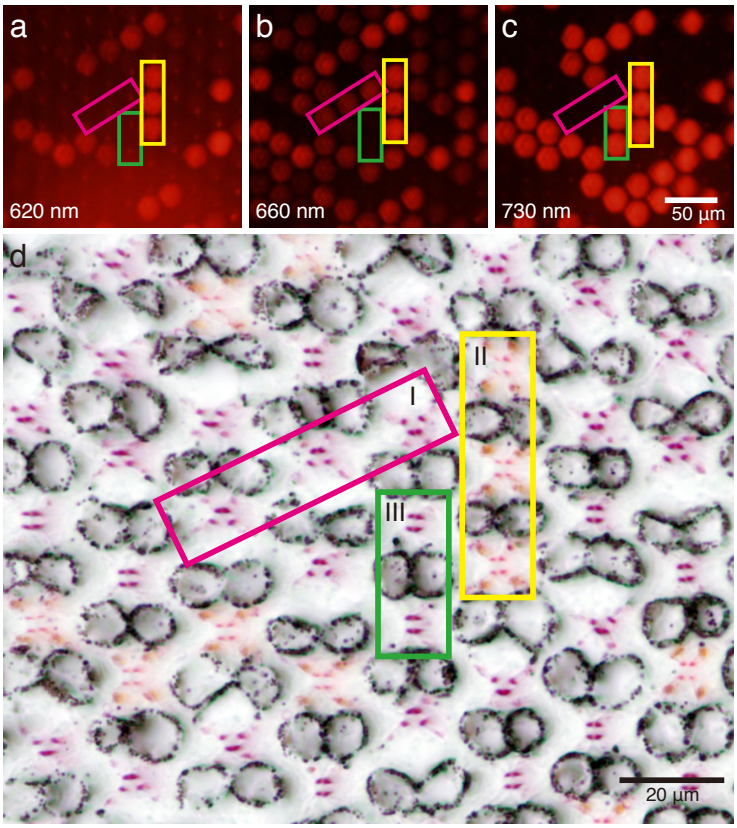

Fig. 1-2. Tapetal reflection and ommatidial pigmentation of ventral region in female *Colias erate*. Red, yellow and green frames indicate each same set of ommatidia. (**a**-**c**) Tapetal reflections of intact eye under epi-illumination. (**d**) Unstained plastic section through the same region of the eye. The reflecting 620 nm to 730 nm ommatidia contain squarely arranged orange pigments around the rhabdom.

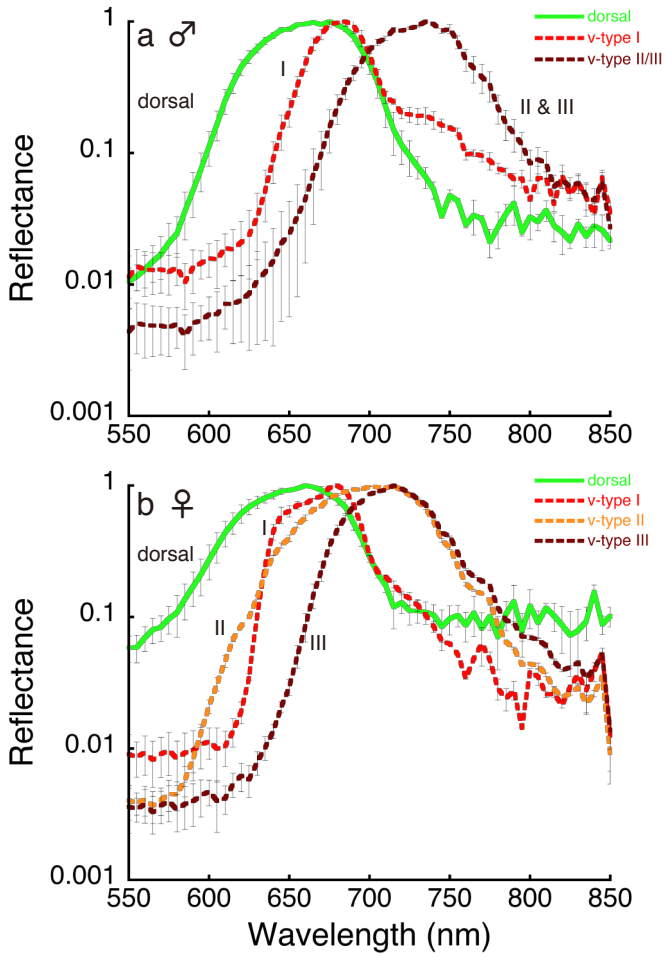

Fig. 1-3. Reflectance spectra of eyeshines from IMSP measurement of males (**a**) and females (**b**). Spectra are shown as medians with standard deviation. According as histological results, reflectance spectra of ventral region (dashed lines) are classified with three ommatidial types.

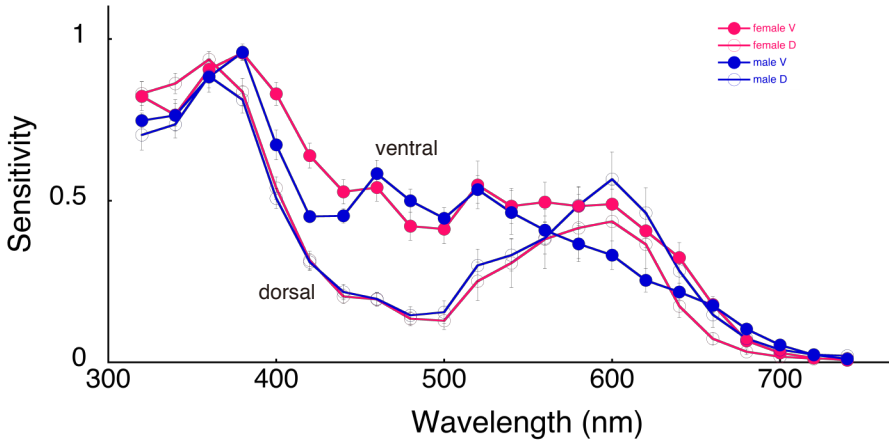

Fig. 1-4. Spectral responses of dorsal (open circle) and ventral (filled circle) region in both sexes by electroretinogram. Spectral response curves are shown as median both in males (blue, n=5) and females (magenta, n=5)

Chapter 2

Coexpression of three middle wavelength-absorbing visual pigments in sexually dimorphic photoreceptors of the butterfly *Colias erate*

This chapter is based on the following paper:

Ogawa Y, Awata H, Wakakuwa M, Kinoshita M, Stavenga DG, Arikawa K (2012) Coexpression of three middle wavelength-absorbing visual pigments in sexually dimorphic photoreceptors of the butterfly *Colias erate*.

Journal of Comparative Physiology A 198: 857-867.

List of abbreviations:

bB, broad-blue; bG, broad-green; CeB, *Colias erate* blue-absorbing opsin; CeL, *Colias erate* long wavelength-absorbing opsin; CeUV, *Colias erate* ultraviolet-absorbing opsin; CeV1, *Colias erate* violet-absorbing opsin 1; CeV2, *Colias erate* violet-absorbing opsin 2; nB, narrow-blue; sB, shouldered-blue

Abstract

The tiered ommatidia of the Eastern Pale Clouded yellow butterfly, *Colias erate*, contain nine photoreceptor cells, four of which contribute their rhabdomeral microvilli to the distal tier of the rhabdom. I analyzed the visual pigments and spectral sensitivities of these distal photoreceptors in both sexes of *Colias erate*. A subset of photoreceptor cells expresses a newly discovered middle wavelength-absorbing opsin, *Colias erate* Blue (CeB), in addition to two previously described middle wavelength-absorbing opsins, CeV1 and CeV2. The other photoreceptors either coexpress CeV1 and CeV2, or exclusively express a short wavelength-absorbing opsin, CeUV, or a long wavelength-absorbing opsin, CeL. Males and females have the same visual pigment expression patterns, but the photoreceptor spectral sensitivities are sexually dimorphic. The photoreceptors coexpressing three middle wavelength-absorbing opsins are broad-blue receptors in males, but in females they are narrow-blue receptors. Those with CeV1 and CeV2 are violet receptors in females, while they are shouldered-blue receptors in males. The sexual dimorphism in spectral sensitivity is caused by a sex-specific distribution of fluorescent pigment that functions as a spectral filter.

Introduction

Visual systems sample the environment with the assembly of retinal photoreceptors. The spectral sensitivity of the photoreceptors is principally determined by the visual pigment absorption spectrum, which depends on the interaction of a protein opsin and retinal, the chromophore. Insects typically have three types of photoreceptors, each expressing an opsin, belonging to the short (S), middle (M) and long (L) wavelength-absorbing classes (Pichaud et al. 1999). For instance, the honeybee has ultraviolet (UV), blue (B) and green (G) receptors, which serve as the basis for their trichromatic system (Wakakuwa et al. 2005).

Compared to honeybees, the eyes of butterflies are much more complicated, because they can be furnished with six (or perhaps more) spectral receptor classes, as was shown for the Japanese swallowtail butterfly *Papilio xuthus* (Arikawa 2003). Butterflies have sophisticated color vision for detecting, for example, nectar-rich flowers or high quality leaves on which to lay their eggs (Kelber and Pfaff 1999; Kinoshita et al. 1999; Koshitaka et al. 2008).

The variety of butterfly photoreceptors is created by a number of different mechanisms. First, spectrally selective filtering pigments modify the spectral sensitivity (Arikawa and Stavenga 1997). Second, opsin genes have undergone repeated duplication events during evolution. For example, pierids (Arikawa et al. 2005; Awata et al. 2009) and lycaenids (Sison-Mangus et al. 2006) have multiple M opsins, and thus have a variety of M receptors. Multiple L opsins exist in *Papilio* and *Parnassius* (Papilionidae) (Kitamoto et al. 1998; Briscoe 2000; Awata et al. 2010), *Helmeuptychia* (Nymphalidae) and *Apodemia* (Riodinidae) (Frentiu et al. 2007a). S opsins are duplicated in *Heliconius* (Briscoe et al. 2010). Third, some photoreceptors coexpress two opsins with different absorption spectra, causing a broad-band spectral sensitivity (Arikawa et al. 2003); these photoreceptors violate the widely-accepted “one photoreceptor - one opsin” principle. Expression of two opsins in a photoreceptor appears to occur more frequently than previously thought (Stavenga and Arikawa 2008). However, coexpression of three or more opsins has so far not been reported, except for a study on salamander cones, using electrophysiological measurements of spectral sensitivities before and after chromatic adaptation. However, no histological evidence was offered (Makino and Dodd 1996).

I have investigated photoreceptor spectral sensitivities in the pierid butterfly *Colias erate* in detail. Among the nine photoreceptors (R1-9) in a *Colias* ommatidium, R1-4 contribute their microvilli to the distal tier of the rhabdom (Fig. 2-1) (Arikawa et al. 2009). At the molecular level, I have identified two M opsins, CeV1 and CeV2, which are coexpressed in a set of photoreceptors. Although the expression pattern is identical among the M opsin-expressing photoreceptors (Awata et

al. 2009), electrophysiological recordings yielded at least four distinct M receptor classes; violet, narrow-blue, blunt broad-blue and sharp broad-blue (Pirih et al. 2010). This discrepancy motivated me to reinvestigate the *Colias* eyes in detail. I thus discovered a novel M opsin, CeB, which is exclusively expressed in a subset of M receptors. In addition I found a clear sexual dimorphism in screening pigments. These findings explain the spectral variability among M receptors in *Colias* eyes.

Materials and Methods

Animals

Adults of the Eastern Pale Clouded yellow butterfly, *Colias erate* Esper, were obtained from a laboratory culture derived from eggs laid by females captured around the Sokendai-Hayama campus, Kanagawa, Japan. Hatched larvae were reared under natural light condition on fresh clover leaves.

Electrophysiology and dye injection

Photoreceptor spectral sensitivities were determined by intracellular recording of responses to monochromatic stimuli provided by a 500 W Xenon arc lamp and a series of narrow-band interference filters ranging from 300 to 740 nm. The light beam was focused on the tip of an optical fiber whose other end was attached to a Cardan arm perimeter device in a Faraday cage, where it provided a point light source (1° in diameter). The quantum flux of each monochromatic stimulus was measured using a radiometer (Model-470D, Sanso, Tokyo, Japan) and adjusted to a standard number of photons using an optical wedge. A butterfly whose wings and legs were removed was fixed on a plastic stage with its dorsal side up and then mounted at the rotation center of the perimeter device. A silver wire inserted into the head served as the indifferent electrode. A glass microelectrode filled with 10 mM Alexafluor 568 (excitation/emission at 576/599 nm), resistance about 100 MΩ, was inserted into the retina through a hole made in the cornea. Membrane potentials were recorded through a preamplifier (MEZ-7200; Nihon Kohden, Tokyo, Japan) connected to a computer via an AD converter (MP-150, BIOPAC Systems, USA). After penetrating a photoreceptor with the electrode, the optical fiber was adjusted to the position yielding maximal photoreceptor responses. First, the spectral type of the impaled photoreceptor was determined by a series of monochromatic flashes of duration 30 ms, spaced 1 s apart. The response-stimulus intensity (V-log I) function was recorded over a 4 log unit intensity range at the photoreceptor's peak wavelength. The V-log I data were fitted to the Naka-Rushton function, $V/V_{max} = I^n/(I^n + K^n)$, where I is the stimulus intensity, V is the response amplitude, V_{max} the maximum response amplitude, K the stimulus intensity eliciting 50 % of V_{max}, and n the exponent. The data were further processed only when V_{max} exceeded 30 mV. At the end of the recording, Alexafluor 568 was injected into the photoreceptor by applying a 2 nA hyperpolarizing current for approximately 5 min.

Anatomy

To correlate the ommatidial auto-fluorescence with pigmentation, I observed an intact eye using a

modified epi-fluorescence telemicroscopic optical assembly (Stavenga 2002) equipped with an objective lens with a large numerical aperture and long working distance (Olympus LUCplanFLN20X, NA 0.45, WD 6.4-7.6 mm). After taking fluorescence pictures under 420 nm excitation, I fixed the eye in 4 % paraformaldehyde in 0.1 mol sodium cacodylate buffer, pH 7.4, at room temperature for 30 min, embedded in Quetol 812 (Nisshin EM, Tokyo, Japan) and made semi-thin transverse sections. I also observed the fluorescence in isolated ommatidia dissociated from the retina by pipetting the tissue in Ringer's solution.

I observed the Alexafluor-injected preparation with a fluorescence microscope (Olympus, BX50) under 550 nm excitation and localized the ommatidium containing the dye-filled photoreceptor. I then made semi-thin sections of the eye as described above, and localized the photoreceptor in the ommatidial array under 550 nm excitation. Subsequently I identified the type of ommatidium by its pigmentation pattern under normal transmission light.

Molecular biology, cloning and phylogeny

Cloning of cDNAs encoding M opsins of *Colias erate* was carried out by a standard protocol. Poly-A RNA was extracted from eyes using QuickPrep micro mRNA puriWcation kit (GE Healthcare, Uppsala, Sweden). To amplify fragments of cDNA encoding opsins of the M classes, I carried out RT-PCR using degenerate primers designed based on consensus sequences of lepidopteran M opsins (see legend of Fig. 2-3). The full-length cDNAs were obtained by 5'- and 3'-rapid amplification of cDNA RACE method. Both PCR and RACE products were puriWed, cloned using TOPO TA cloning kit (Invitrogen, Carlsbad, CA) and sequenced using ABI3130xl and BigDye terminator v1.1 (Applied Biosystems, Warrington, UK). The obtained sequences were aligned with known sequences and processed for phylogenetic analysis by the maximum parsimony and the neighbor-joining protocols using the MEGA 4.0.1 software (Tamura et al. 2007) and also by the maximum likelihood protocol using the PHYML 2.4.4 software (Guindon et al. 2005). For comparison, I also analyzed the M opsins of other species in the subfamily Coliadinae (*Eurema hecabe*, *Eurema laeta, Gonepteryx rhamni, Catopsilia pomona*).

In situ hybridization

Isolated eyes immersed in 4% paraformaldehyde in 0.1 M phosphate buffer (pH 7.2) were microwave-irradiated six times for 5 s each (total 30 s) and then fixed for 20 min at 4°C. After dehydrating with graded ethanol, the eyes were sequentially in filtrated with terpineol and xylene, embedded into Paraplast (Sigma-Aldrich, St Louis, MO, USA) and sectioned at 8 μm thickness. The

sections were deparaffinized with xylene, treated with 10 μg/ml proteinase K in PBS for 5 min at 37°C and acetylated with 0.25% acetic acid in 0.1 M triethanolamine (pH 8.0) for 10 min prior to hybridization. Antisense RNA probes were synthesized from linearized plasmid carrying partial sequence of identified opsin mRNAs by in vitro transcription using digoxigenin-UTP (Roche, Mannheim, Germany). The probes were denatured at 70°C for 10 min before adding hybridization solution (300 mM NaCl, 2.5 mM EDTA, 200 mM Tris–HCl, pH 8.0, 50% formamide, 10% dextran sulfate, 1 mg/ml yeast tRNA, and 1X Denhardt's solution), and again treated at 90°C for 5 min after being diluted with the hybridization solution at the final concentration of 0.5 μg/ml. The heat-treated probe was applied to the sections at 45°C overnight. After washing in 2X SSC at 55°C for 15 min and then 50% formaldehyde-2X SSC at 55°C for 2 h, the sections were subsequently treated with 10 μg/ml RNase A for 1 h at 37°C and with 0.5% blocking solution (Roche, Mannheim, Germany) for 30 min at room temperature. The hybridized probes were detected using anti-digoxigenin- AP Fab fragments (Roche, Mannheim, Germany) and then visualized using 4-nitroblue tetrazolium chloride and 5-bromo-4-chloro-3-indolyl phosphate for light microscopy.

Modeling

To quantitatively describe the spectral sensitivities of distal photoreceptors of *Colias erate*, I constructed an optical simulation model which incorporated the anatomical details of the ommatidia (Arikawa et al. 2009). The assumptions were as follows. The length of the distal tier of the rhabdom, consisting of the four rhabdomeres of photoreceptors R1-4, was 250 μm in type I and 200 μm in type II and III ommatidia. The most distal 80 μm of the rhabdoms of type I ommatidia of the male and type II ommatidia of the female contain a fluorescent pigment. Its absorbance spectrum was assumed to be identical to that of the fluorescent pigment in the rhabdoms of the small white butterfly, *Pieris rapae* (Arikawa et al. 2005). The possible contributions of the cluster of perirhabdomal pigments as well as of the reflecting tapetum were ignored, because previous studies on *Pieris* demonstrated that their effect on the spectral sensitivity of the distal photoreceptors was negligible (Wakakuwa et al. 2004; Stavenga and Arikawa 2011). Visual pigment absorption spectra were calculated using the Govardovskii template (Govardovskii et al. 2000). I applied the simple model approach of Stavenga and Arikawa (2011) and thus neglected the wave-optical properties of the dioptric system and rhabdom. The transmittance of a rhabdom layer with thickness Δz then is given by

$$T(\lambda) = \exp\left[-\kappa(\lambda)\Delta z\right] \tag{1}$$

with

$$\kappa(\lambda) = \kappa_V(\lambda) + \kappa_S(\lambda) \tag{2}$$

where κ_V is the local absorbance coefficient due to absorption by the visual pigments, which is given by

$$\kappa_V = \kappa_{V,max}\left\{\sum \alpha_i(\lambda)\rho_i\right\} \tag{3}$$

where $\kappa_{V,max}$ is the peak absorbance coefficient, α_i is the normalized absorbance spectrum of the visual pigment in photoreceptor R_i (i = 1-4), and ρ_i is the occupation ratio of the rhabdomere of R_i in the rhabdom. κ_S is the absorbance coefficient of the fluorescent pigment,

$$\kappa_S = \kappa_{S,max}\alpha_S(\lambda) \tag{4}$$

with $\kappa_{S,max}$ the peak absorbance coefficient and α_S the normalized absorbance spectrum of the fluorescent pigment. The light flux at location z, $I(z,\lambda)$, is then transformed into that at location $z + \Delta z$, $I(z + \Delta z)$, by

$$I(z + \Delta z, \lambda) = T(\lambda)I(z, \lambda) \tag{5}$$

The light flux absorbed by the visual pigment of the individual photoreceptors in a compartment of thickness Δz is given by

$$\Delta A_i(\lambda) = \left[I(z, \lambda) - I(z + \Delta z, \lambda)\right]\kappa_{V,max}\alpha_i(\lambda)\rho_i / \kappa(\lambda) \tag{6}$$

I assumed that at all wavelengths a unit light flux entered the ommatidia. Before reaching the photoreceptors, the incident light first passes the dioptric apparatus, consisting of the corneal facet lens and crystalline cone. I assumed that the transmittance of the dioptric apparatus was equivalent to that of the moth *Endromis* (Bernhard et al. 1965). Its transmittance spectrum, $T_C(\lambda)$, is thus identical to the relative light flux spectrum $I_0(\lambda)$ at z = 0 μm, the tip of the rhabdom. Summing the absorbed light fractions of the individual photoreceptors over the different rhabdom compartments then yields the photoreceptor's absorbance spectrum. Normalizing this yields the spectral sensitivity.

Results

Sexual dimorphic ommatidia

The compound eye of *Colias erate* consists of about 6500 ommatidia, each containing nine photoreceptor cells, R1-9. They extend photoreceptive microvilli to form a tiered and fused rhabdom (Fig. 2-1). R1-4 contribute their microvilli to the distal tier of the rhabdom, and therefore are called the distal photoreceptors. The R5-8 microvilli form the proximal tier of the rhabdom and thus R5-8 are the proximal photoreceptors. The basal photoreceptor R9 adds a few microvilli at the base of the rhabdom (Arikawa et al. 2009). The ommatidia of *Colias* can be divided into three types, I-III, which are distinguishable by their characteristic patterns of perirhabdomal pigmentation. In a previous study (Arikawa et al. 2009) it was concluded that the perirhabdomal pigments of all three ommatidial types have the same red color and that type I ommatidia contain a strongly fluorescent pigment. However, in the present study I found that this organization only holds for the male eye (Fig. 2-2a). In female eyes the perirhabdomal pigments of ommatidial types I and III have the same red color as the pigment clusters of males, but in ommatidial type II the pigment is orange. The fluorescent pigment is not expressed in type I, as in the male, but in type II ommatidia (Fig. 2-2b). Fluorescence and transmission light microscopy of an isolated ommatidium demonstrated that the fluorescent pigment is concentrated in the most distal 80 μm-region of the rhabdom (Fig. 2-2c).

Identification of CeB, a new middle wavelength-absorbing opsin

I discovered a new opsin-like sequence in addition to the four opsin mRNAs previously identified in the *Colias* retina. Figure 2-3 shows a phylogenetic relationship of M opsins of butterflies. The newly identified sequence appeared to be close to PrB, the blue-absorbing visual pigment of *Pieris rapae* (λ_{max} = 450 nm). I therefore termed the opsin CeB (*Colias erate* Blue). CeV1 and CeV2 both share the same root as PrV, the violet-absorbing visual pigment of *Pieris* (λ_{max} = 420 nm).

In addition to *Colias erate*, I investigated the presence of M opsins in a few related butterflies. I thus obtained full V1, V2 and B opsin orthologs from the eyes of *Eurema hecabe* and *Gonepteryx rhamni* (Fig. 2-3). I identified partial sequences of three orthologs in *Catopsilia pomona* (CatpB, AB721365; CatpV1, AB721366; CatpV2, AB721367) and *Eurema laeta* (ElB, AB721373; ElV1, AB721374; ElV2, AB721375). These findings suggest that butterflies of the subfamily Coliadinae generally possess three opsins of the M opsin class.

Distribution of CeB in the retina

I localized the CeB mRNA in the retina by *in situ* hybridization and correlated the labeling with the previously identified distribution of the S (CeUV), M (CeV1, CeV2) and L (CeL) opsin (Awata et al. 2009). I labeled transverse sections of the distal retina with probes specific to the CeUV, CeV1 and CeB mRNAs.

Figure 2-4 shows three consecutive histological sections of an area containing both the dorsal and ventral eye regions (Fig. 2-4a-c). The CeUV probe labeled both R1 and R2 of type III ommatidia, but it labeled exclusively either R1 or R2 in type I ommatidia (Fig. 2-4a). The CeV1 probe labeled the opposite R2 or R1 in type I ommatidia (Fig. 2-4b). The CeV1 probe labeled both R1 and R2 in type II ommatidia, but the labeling was strong in the dorsal region and faint in the ventral region. The CeB probe exclusively labeled R1 and R2 photoreceptors of type II ommatidia (Fig. 2-4c) in the ventral region (type II_V), but not in the dorsal region (type II_D). Interestingly, I detected labeling of the R2 photoreceptors in type II ommatidia in the transition area between the dorsal and ventral regions (type II_T). In the R2 of type II_T, the labeling with the CeV1 probe was slightly weaker than in the R1 where no CeB labeling was detected. Because CeV1 and CeV2 are always simultaneously expressed, the CeB expressing photoreceptors of type II_T and II_V ommatidia coexpress three opsin mRNAs, CeB, CeV1 and CeV2 (Fig. 2-4d).

In summary, of the nine photoreceptors, R1-9, the distal photoreceptors R1 and R2 express mRNAs of S and/or M opsins in three fixed combinations in the ventral region (Table 2-1). The R3-8 in all ommatidia appeared to express the long-wavelength absorbing CeL (not shown). I found no distinct difference in the opsin expression patterns of male and female.

Spectral sensitivities of distal photoreceptors

I measured the spectral sensitivities of the distal photoreceptors, R1-4, in all three types of ommatidia in the ventral region of both male and female eyes. Among more than 200 recordings, 70 photoreceptors were successfully labeled and thus analyzed in the present study. According to their sensitivity profiles, I categorized the photoreceptors into three classes, S, M and L.

I specifically focused my attention on the M receptors, because their spectral sensitivity appeared to vary widely and they were clearly sexually dimorphic. Figure 2-5 shows four examples of labeled photoreceptors. The top row shows the spectral sensitivity of Alexafluor-filled photoreceptors (middle row), which were localized in the ommatidial array by regular transmission light microscopy (bottom row), I identified receptors with a shouldered-blue (sB) spectral sensitivity, peaking at 440 nm with a kink at 420 nm (Fig. 2-5a). These were either R1 or R2 photoreceptors,

located at the longer side of the trapezoidal pigment cluster in type I ommatidia of males. The corresponding photoreceptors of female eyes were violet (V) receptors (Fig. 2-5b). I also recorded broad-blue (bB) receptors, with spectral sensitivity peaking at 460 nm, bandwidth about 100 nm. These were male-specific R1 and R2 photoreceptors located in type II ommatidia (Fig. 2-5c). The corresponding photoreceptors of females were narrow-blue (nB) receptors, peaking at 480 nm, with reduced sensitivity below 420 nm (Fig. 2-5d).

The S class (UV) receptors (labeling data not shown) were maximally sensitive at 360 nm, with spectral bandwidth of about 60 nm (Fig. 2-6a, c, d, f). In type I ommatidia of both sexes, the UV receptors were either the R1 or R2 located on the shorter side of the trapezoidal pigment cluster. In type III ommatidia, also of both sexes, R1 as well as R2 was UV sensitive (Fig. 2-6c, f).

The R3 and R4 photoreceptors of all ommatidial types in both sexes were L receptors, with maximal sensitivity in the green wavelength region, around 560-580 nm (Fig. 2-6). The R3 and R4 of male type I ommatidia were termed broad-green (bG) receptors (Table 2-1), because their spectral sensitivity (bandwidth ~140 nm), was distinctly broader than that of the green (G) receptors of ommatidial types I and III bandwith ~100 nm).

Model calculation

To quantitatively understand the spectral sensitivities, I calculated the light flux in the rhabdom and the resulting photoreceptor sensitivity spectra with an optical simulation model. I assumed that at all wavelengths a unit light flux entered the ommatidia. Before reaching the photoreceptors, the incident light first passed the dioptric apparatus, consisting of the corneal facet lens and crystalline cone. I assumed that the transmittance of the dioptric apparatus was equivalent to that of the moth *Endromis* (Bernhard et al. 1965). Its transmittance spectrum, $T_C(\lambda)$, is thus identical to the relative light flux spectrum $I_0(\lambda)$ at $z = 0$ μm, the tip of the rhabdom. The spectra shown in Fig. 2-6 were obtained by using a peak absorbance coefficient $\kappa_{V,max} = 0.005$ μm^{-1} for all visual pigments. I took $\kappa_{S,max} = 0.02$ μm^{-1} for the peak absorbance coefficient of the fluorescent pigment in male type I and female type II ommatidia.

The spectral sensitivities of UV receptors in type I and III ommatidia of both sexes (Fig. 2-6a, c, d, f) were well reproduced by postulating a rhodopsin absorption spectrum peaking at 360 nm (R360). Similarly the sensitivities of G receptors were explained reasonably well by assuming a rhodopsin R565 (Fig. 2-6a-f).

I found that the variety of spectral sensitivities obtained for the M receptors (Fig. 2-5) results from the complex participation of three visual pigments and the fluorescent pigment (Fig.

2-6a, b, d, e). The V receptor of female type I ommatidia, where CeV1 and CeV2 are expressed, was well reproduced by assuming an unfiltered rhodopsin peaking at 430 nm (Fig. 2-6d). I therefore modeled both CeV1 and CeV2 as a rhodopsin R430. I could reproduce the sB sensitivity of male type I ommatidia (Fig. 2-6a) well by assuming that the fluorescent pigment of those ommatidia acts as an optical filter with peak absorption at 416 nm (Arikawa et al. 2005).

The M receptors (bB and nB) in type II_V ommatidia express three opsins, CeV1, CeV2 and CeB. By combining a rhodopsin R430 (CeV1 and CeV2) together with a rhodopsin R460 (CeB), with ratio 2:8, the spectral sensitivity of male bB photoreceptors of type II ommatidia could be well reproduced (Fig. 2-6b). For mimicking the spectral sensitivity of the nB receptors of the female, also in type II ommatidia (Fig. 2-6e), I assumed that the same visual pigments are expressed with the same ratio as in the male and that the only difference was the short-wavelength absorbing fluorescent pigment acting as a violet optical filter, resulting in a reduced sensitivity at short wavelengths (Fig. 2-6e).

Discussion

In my analysis of the distal retina of *Colias erate*, I found a new M opsin, CeB, which is expressed together with two other M opsins in a specific class of photoreceptor cells, namely the R1 and R2 photoreceptors of type II ommatidia in the ventral eye of both sexes (Table 2-1). Whereas males and females appear to have the same visual pigment expression patterns, I found a remarkable sexual dimorphism in the retinal pigmentation, which functions in sex-specific tuning of the photoreceptor spectral sensitivities.

Evolution of middle wavelength-absorbing opsins in Pieridae

In a previous study of the visual pigments of *Colias erate*, two opsins in the insect M clade, CeV1 and CeV2, were identified (Awata et al. 2009). Both clustered with the violet opsin of *Pieris rapae*, PrV (Fig. 2-3). Orthologs of the *Pieris* blue opsin PrB were not detected in *Colias*, which has led them to the conclusion that the B opsin ortholog was somehow lost in the lineage of Coliadinae (Wakakuwa et al. 2010). However, the large variety of spectral sensitivities of M receptors of *Colias* found in a subsequent study (Pirih et al. 2010) could not be explained with the visual pigments then known, and I therefore carried out an extensive search for additional M opsins in *Colias*. As I have reported here, this yielded the discovery of a novel opsin, CeB, which clustered with the PrB opsin of *Pieris rapae* (Fig. 2-3). I also found that other Coliadinae species, *Eurema hecabe, Eurema laeta, Gonepteryx rhamni* and *Catopsilia pomona*, have three M opsins, which cluster with CeV1, CeV2 and CeB (Fig. 2-3).

The present phylogeny indicates that in an early stage of evolution of the family Pieridae, an M opsin gene duplicated in a common ancestor of the subfamilies Pierinae and Coliadinae, eventually forming B and V opsins. In the lineage of Coliadinae, the V opsin again duplicated, forming V1 and V2, while the B opsin remained unduplicated.

Origin of spectral sensitivity of distal photoreceptors

The eyes of *Colias* consist of three types of ommatidia with tiered rhabdoms (Fig. 2-1). Here I focused on the four photoreceptors comprising the distal tier, R1-4, with the specific aim of understanding the spectral variability of the R1 and R2 photoreceptors in the ventral retina. The *in situ* hybridization results of the male and female were identical: a specific set of R1 and R2 photoreceptors simultaneously expressed CeV1, CeV2 as well as CeB (Fig. 2-4). On the other hand, I found sexual dimorphism in the ommatidial fluorescence (Fig. 2-2) and in the spectral sensitivities

of the distal photoreceptors (Fig. 2-5). Evidently the sexual dimorphism in photoreceptor sensitivity is caused by the fluorescent pigment, which acts as an optical filter.

The molecular phylogeny (Fig. 2-3) and the expression analysis of PrV and PrB of *Pieris* (Wakakuwa et al. 2010) suggested that the absorption spectra of CeV1 and V2 are similar to PrV (R420) and that the absorption spectrum of CeB resembles that of PrB (R450). I used the R420 and R450 spectra in my initial optical simulation modeling, but to achieve satisfactory fits with the measured spectral sensitivities I had to slightly modify the visual pigment absorption spectra, yielding R430 and R460.

In type I ommatidia, R1 or R2 on the longer side of the pigment trapezoid coexpress CeV1 and CeV2. In females these photoreceptors are of the V type (Fig. 2-4b, Fig. 2-6d). The model straightforwardly reproduced the V receptor sensitivity by assuming that both CeV1 and CeV2 are 430 nm-absorbing visual pigments (R430, Fig. 2-6d). The cells in the same location in males are sB receptors, which have an enhanced sensitivity tail in the UV with a shoulder at around 420 nm (Figs 2-4a and 2-6a). This sexual dimorphism is attributable to the filtering effect of the fluorescent pigment in the male type I ommatidia (Fig. 2-5a). The fluorescent pigment exists in the distal portion of the rhabdom (Fig. 2-5c) where it absorbs violet light and emits greenish fluorescence: for the photoreceptors in the corresponding ommatidia, this light-absorbing property acts as a strong filter while the contribution of the weak fluorescence to the photoreceptors' spectral sensitivities is negligible. The fluorescent pigments in the eyes of *Papilio xuthus* (Arikawa et al. 2003) and the male *Pieris rapae* (Arikawa et al. 2005) thus act similarly.

While males have the fluorescent filter in type I ommatidia, in females the fluorescent pigment exists in type II ommatidia (Fig. 2-2). R1 and R2 of type II ommatidia express three opsin mRNAs, CeV1, CeV2 and CeB in both sexes. By assuming that both CeV1 and V2 are R430 and CeB is a R460, the model successfully reproduced the sensitivity of the bB receptors in males. This indicates that all three visual pigments are functional (Fig. 2-4c, 2-6b). In females, the corresponding photoreceptors are nB receptors, whose sensitivity spectrum was well reproduced by combining the filtering effect of the fluorescent pigment with an absorption spectrum peaking at 416 nm (Arikawa et al. 2005). Presumably, in the evolutionary process, opsin duplication happened first and the sexually dimorphic distribution of the fluorescent filter came into existence later. The resulting difference in photoreceptor spectral sensitivities is probably related to the sexually dimorphic wing colors of this species.

Since the broad-band receptor in *Papilio*, which is the result of coexpression of a green and a red visual pigment, was demonstrated (Arikawa et al. 2003) in one and the same class of

photoreceptor cell, several examples of visual pigment coexpression have been reported in invertebrates (Sison-Mangus et al. 2006; Jackowska et al. 2007; Mazzoni et al. 2008; Rajkumar et al. 2010). Coexpression of two visual pigments is also well-documented for vertebrates (Archer and Lythgoe 1990; Roehlich et al. 1994; Loew et al. 1996; Makino and Dodd 1996; Applebury et al. 2000; Cheng and Novales Flamarique 2004). The present study provides the first example of coexpression of three opsins in invertebrates. One uncertainty is that the spectral sensitivities could be reproduced without postulating different absorption spectra for CeV1 and CeV2, which could mean that either CeV1 or CeV2 is non-functional. However, in preliminary ectopic expression studies of CeV1 and CeV2 in *Drosophila*, both sequences appeared to be able to construct functional visual pigments. Presumably therefore, the CeV1 and CeV2 of *Colias erate* are presently in the evolutionary process of functional diversification. A comparative study in other Coliadinae species may provide further insight into whether and how the duplicated opsins have enhanced the animals' visual capacity.

Many of these examples of coexpressed opsins were duplicated rather recently in the evolutionary process: they cluster in the same clade (Fig. 2-3). This also holds for *Colias*. However sometimes coexpressed opsins belong to different clades. In the Apollo butterfly (*Parnassius*), an S and M opsin are coexpressed (Awata et al. 2010), while coexpression of an M and L opsin has been found in a rodent (Roehlich et al. 1994) and in the lycaenid butterfly, *Lycaena rubidus* (Sison-Mangus et al. 2006). The evolutionary history of the coexpression of opsins from different clade is probably more complicated than for coexpression from the same clade. Elucidation of these processes deserves further analysis.

Dorso-ventral specialization

The above discussion applies to the ventral region of *Colias*, which occupies about two thirds of the eye. It is distinct from the dorsal region, comprising the remaining third of the eye(Arikawa et al. 2009; Awata et al. 2009). The dorsal region should not be confused with the so-called dorsal rim area. This area is made up of just a few ommatidial rows along the dorsal edge of the compound eye. The dorsal rim area has not yet been explored in *Colias*, but it is probably specialized for polarized light detection, as in many insects (Kolb 1986; Horvath and Varju 2004; Labhart et al. 2009).

The dorsal eye region of *Colias* is characterized by a reduced level of perirhabdomal pigment (Arikawa et al. 2009) and an absence of the fluorescent pigment. Among the results presented in this study, the border between the dorsal and ventral regions is clearest in the *in situ* hybridization with the CeB probe, which strongly labels type II ommatidia in the ventral region (Fig.

2-4c). The CeV1 probe labels the R1 and R2 of type II ommatidia in the dorsal region more strongly than in the ventral region (Fig. 2-4b). The R1 and R2 of dorsal type II ommatidia (II_D in Fig. 2-4) are not labeled by the CeB probe. In the dorsal region of males I in fact encountered photoreceptors with spectral sensitivity similar to that of the female-specific V receptors: these are probably R1 and R2 of type II_D ommatidia, which are non-fluorescent and thus have no optical filter. In the transitional area between the dorsal and ventral regions, I found type II ommatidia with R2 labeled with the CeB probe (II_T in Fig. 2-4). These receptors presumably have a spectral sensitivity intermediate between that of V and bB receptors. The present results suggest that the dorsal eye region has no sexual dimorphism and a fairly simple organization of the distal tier of the ommatidia, with only UV, V and G receptors. The spectral properties of the proximal photoreceptors, R5-8, will be treated elsewhere.

Figures

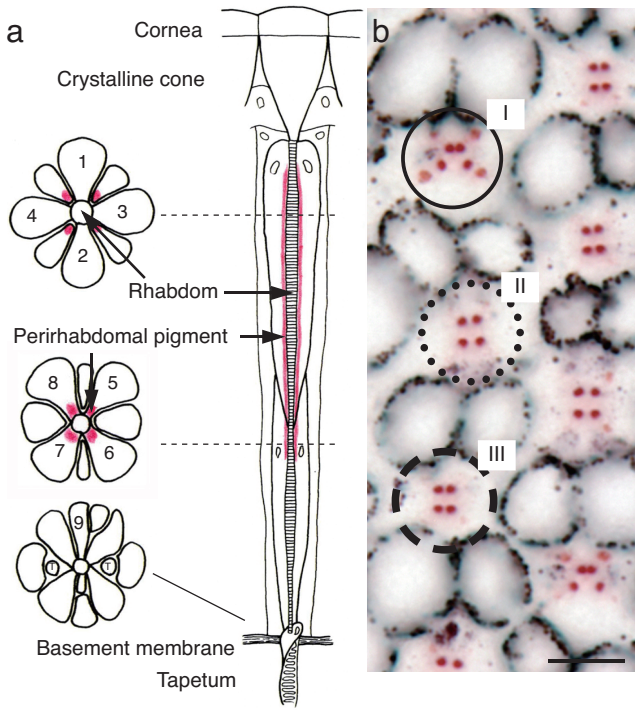

Fig. 2-1. Anatomy of a *Colias* ommatidium. (**a**) Schematic diagram of a *Colias* ommatidium. Transverse views at three depths (left) at levels indicated in the longitudinal view (right). The numbers denote the nine photoreceptors, R1-9; T, tracheole. The rhabdom is surrounded by four clusters of screening pigment, which are located in R5-8. (**b**) LM image demonstrating three ommatidial types; unstained plastic transverse section through the distal tier of the ventral portion of a male eye. The different arrangements of the four pigment clusters around the rhabdom characterize the three types of ommatidia: type I (trapezoidal, solid circle), type II (square, dotted circle) and type III (rectangular, dashed circle). Scale bar: 10 μm.

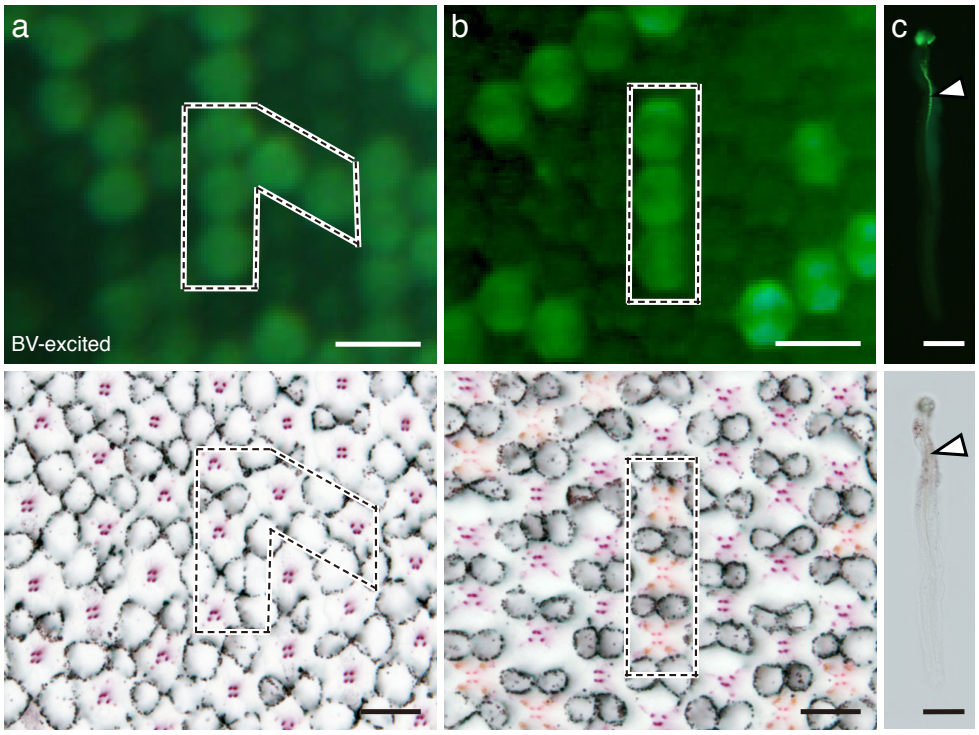

Fig. 2-2. Sexual dimorphic distribution of fluorescent and perirhabdomal pigments (**a**, male; **b** female). Blue-violet (420 nm) excited fluorescence in intact eyes (top) and unstained plastic section of the same eyes (bottom). Dashed frames indicate identical sets of fluorescent ommatidia. The fluorescent ommatidia are trapezoidal type I in male (**a**) and square type II in female *Colias erate* (**b**). (**c**) An isolated ommatidium of male under blue-violet excitation (top) and in transmitted light (bottom). The arrowhead indicates the distal region where the rhabdom contains a fluorescent pigment. Scale bars: 50 μm in top of **a** and **b**; 20 μm in bottom of **a** and **b**; 50 μm in **c** (top and bottom).

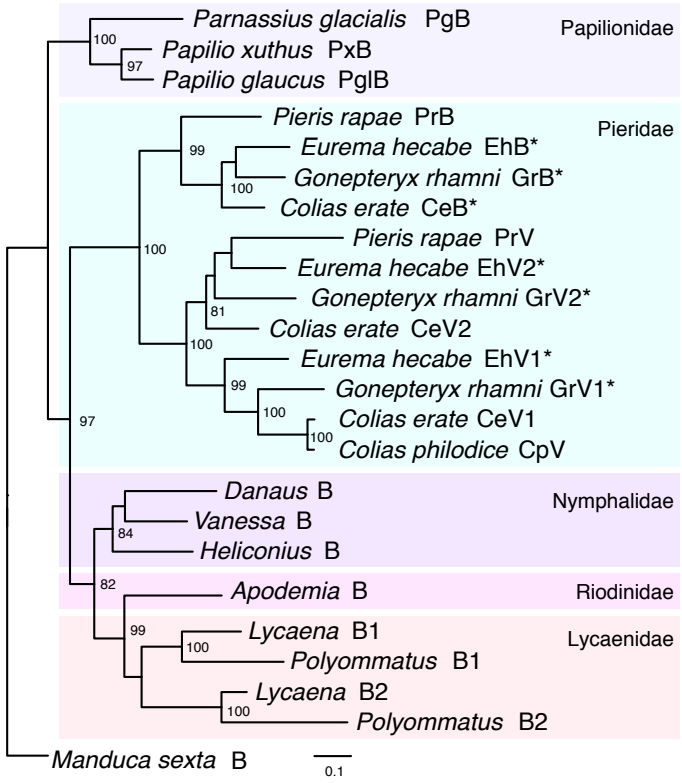

Fig. 2-3. Phylogenetic relationship of opsins of middle wavelength-absorbing visual pigments of butterflies produced by the maximum likelihood protocol. The numbers at the nodes indicate % posterior probability. The nodes without the values have the probabilities of less than 80%. The asterisks indicate that the visual pigments are first described in this study: accession numbers of them are AB721364 (CeB), AB721368 (EhB), AB721369 (EhV1), AB721370 (EhV2), AB721376 (GrB), AB721377 (GrV1) and AB721378 (GrV2). To search for the B opsins, I used three forward (B0-1F, -2F, -3F) and two reverse (PapilionoideaB-1R, -2R) degenerate primers, all based on lepidopteran M opsins. The sequences are as follows:

B01_F: TACTAGTATHGGICCNATGGCNTAYCC,

B02_F: CACTAGTGGITGGAAYATHCCNGARGARC

B03_F: TACTAGTAAYGGIATHGTNATHTGG

PapilionoideaB-1R: ACRTTCATYTTYTTNGCYTG

PapilionoideaB-2R: GCRTAIACCCANGGRTCDAT

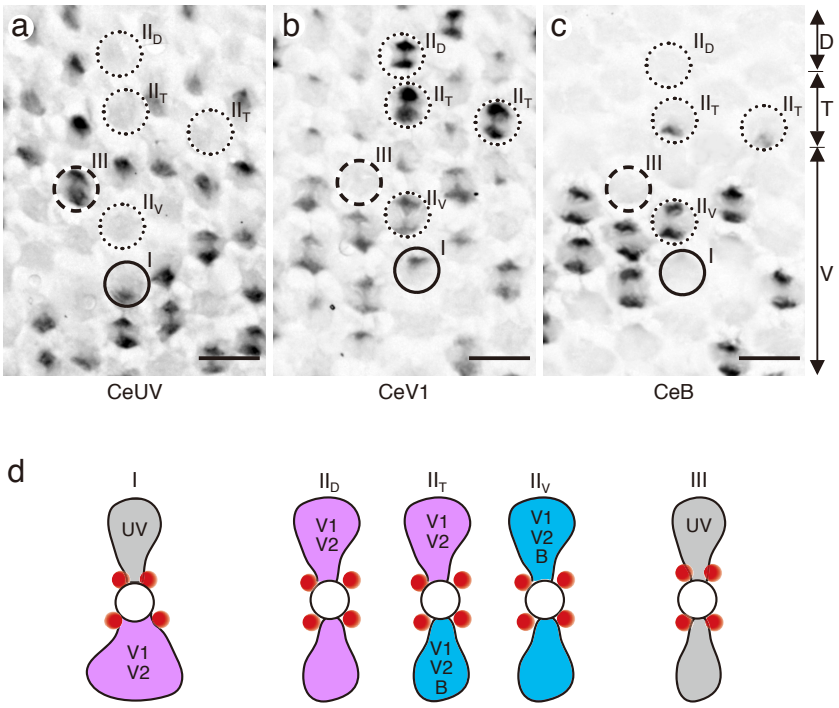

Fig. 2-4. Expression patterns of the CeUV, CeV1 and CeB opsins. Three consecutive transverse histological sections of the middle region of the eye, including a small dorsal (D) part, a transitional area (T) and several ommatidial rows of the ventral area (V). The sections were labeled with specific probes of CeUV (**a**), CeV1 (**b**) and CeB (**c**). The ommatidial types were identified by normal transmission light microscopy (see **Fig. 2-2**; type I: solid circles; type II: dotted circles; type III: dashed circles). The type II ommatidia are divided into II_D (dorsal), II_T (transitional), and II_V (ventral), based on labeling with the probe of the novel blue opsin, CeB; only in ventral ommatidia were R1 and R2 distinctly labeled, whereas those in dorsal ommatidia were not, and intermediate labeling occurred in the transitional area. (**d**) Diagram of the labeling pattern of the R1 and R2 receptors, which express S (UV) and M (V1, V2 and B) opsins.

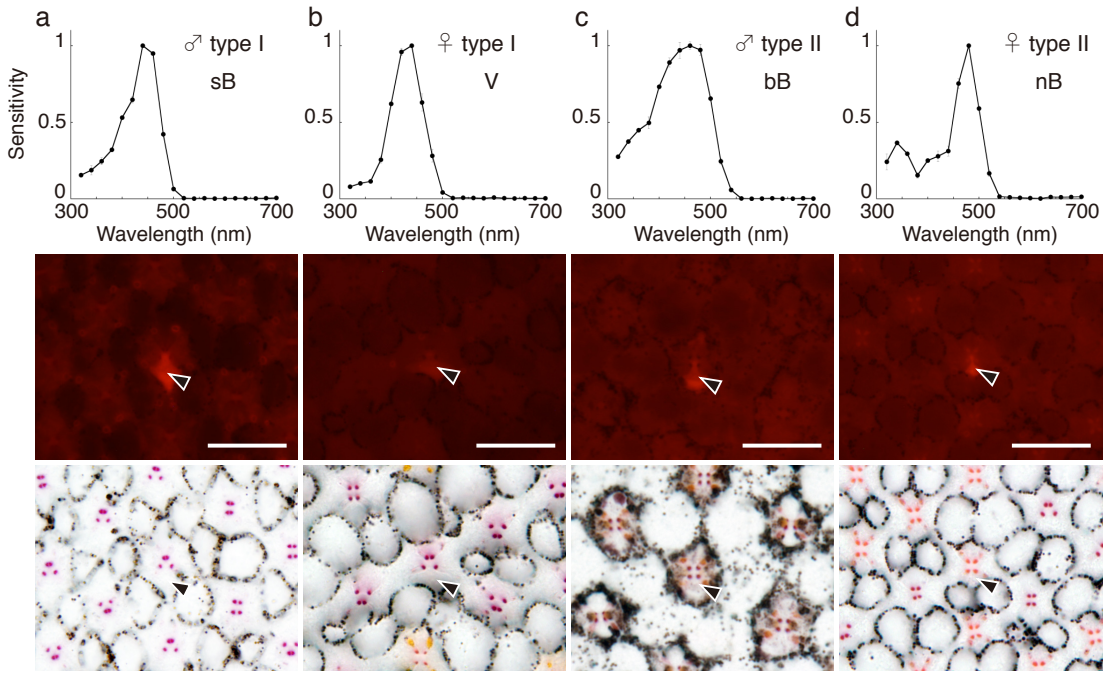

Fig. 2-5. Spectral sensitivity (top row, mean ± standard errors) and localization (arrowheads in middle and bottom rows) of M receptors. (**a**) Shouldered-blue (sB) receptor in a male type I ommatidium. (**b**) Violet (V) receptors in a female type I ommatidium. As with the sB cell of males, this cell is localized on the longer side of the trapezoidal pigment cluster. (**c**) Broad-blue (bB) receptor in a male type II ommatidium. (**d**) Narrow-blue (nB) receptor in a female type II ommatidium. Scale bars: 20 μm.

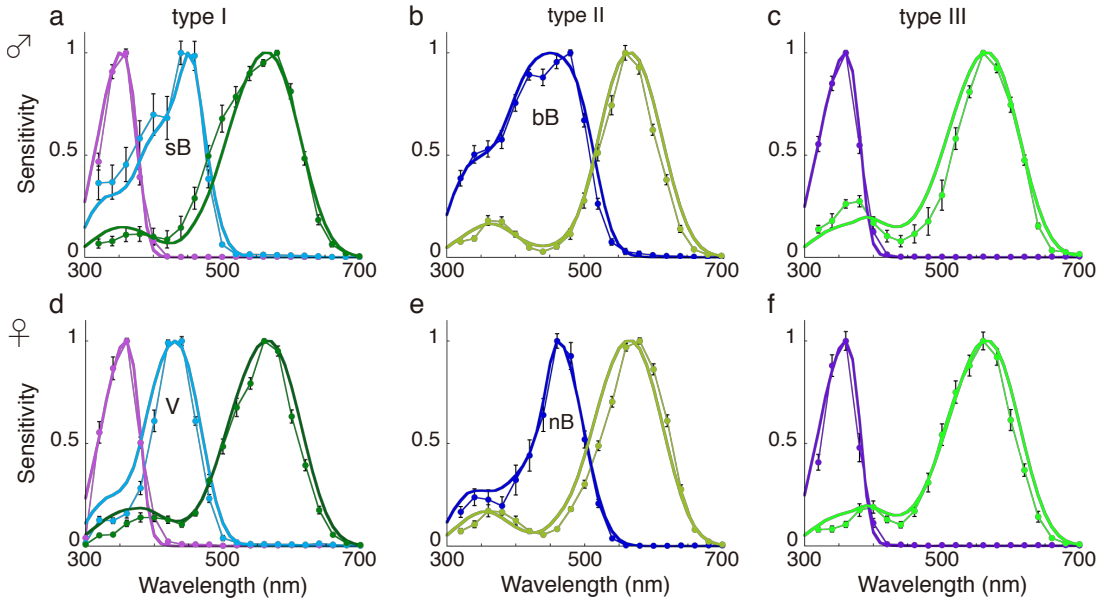

Fig. 2-6. Spectral sensitivities of distal photoreceptors and model calculations. The average spectral sensitivity (n = 5 in all receptors, mean ± standard errors) for male (**a**-**c**) and female (**d**-**f**) ommatidia of type I (**a**, **d**), type II (**b**, **e**), and type III (**c**, **f**) are shown together with spectra calculated using a simple rhabdom model.

Pigment			Fluorescence	R1	R2	R3/4
I	Trapezoid	♂	+	UV	sB	bG
		♀	–	UV	V	G
		opsin mRNA		*CeUV*	*CeV1, V2*	*CeL*
II_V	Square	♂	–	bB		G
		♀	+	nB		G
		opsin mRNA		*CeV1, V2, B*		*CeL*
III	Rectangular	♂, ♀	–	UV		G
		opsin mRNA		*CeUV*		*CeL*
II_D	Square	♂, ♀	–	V(?)		G
		opsin mRNA		*CeV1, V2*		*CeL*
II_T	Square	♂	–	V(?)	bB(?)	G
		♀	?	V(?)	nB or bB	G
		opsin mRNA		*CeV1, V2*	*CeV1, V2, B*	*CeL*

Table 2-1. Summary of the characteristics of the distal photoreceptors in the three ommatidial types in the ventral region of the eye of *Colias erate*. Question marks for II_D and II_T types (lower 2 rows) indicate uncertainty

Chapter 3

Sex-specific retinal pigmentation results in sexually dimorphic long-wavelength-sensitive photoreceptors in the Eastern Pale Clouded Yellow butterfly, *Colias erate*

This chapter is based on the following paper.

Ogawa Y, Kinoshita M, Stavenga DG, Arikawa K (2013)

Sex-specific retinal pigmentation results in sexually dimorphic long-wavelength-sensitive photoreceptors in the Eastern Pale Clouded Yellow butterfly, *Colias erate*.

Accepted by the Journal of Experimental Biology.

Abstract

The compound eyes of the Eastern Pale Clouded Yellow butterfly, *Colias erate*, contain three types of ommatidia (I, II and III), identifiable by the differing arrangements of pigment clusters around the rhabdoms. The pigment color is red in all ommatidial types except for type II ommatidia of females, where the pigment is orange. Intracellular recordings demonstrated that the spectral sensitivities of the proximal photoreceptors (R5-8) of all ommatidia in both sexes are strongly tuned by the perirhabdomal pigments. These pigments act as long-pass filters, shifting the peak sensitivities into the wavelength range above 600 nm. Due to the sex-specific pigments in type II ommatidia, the spectral sensitivities of the R5-8 photoreceptors of females peaked at 620 nm while those in males peaked at 660 nm. The measured spectral sensitivities could be well reproduced by an optical model assuming a long-wavelength-absorbing visual pigment with peak absorbance at 565 nm. Whereas the sexual dimorphism was unequivocally demonstrated for the ventral eye region, dimorphism in the dorsal region was not found. Presumably the ventral region is adapted for sexual behaviors such as courtship and oviposition.

Introduction

The eyes of butterflies are composed of thousands of ommatidia, each containing nine photoreceptor cells, R1-9. The visual pigment-containing organelles of these photoreceptors, the rhabdomeres, are closely apposed and thus form a fused rhabdom. In many butterflies, specifically pierids and papilionids, the rhabdom is tiered. The distal tier is made up by the rhabdomeric microvilli of four distal photoreceptors (R1-4), and the proximal tier consists of the microvilli of four proximal photoreceptors (R5-8). At the base of the rhabdom, the basal photoreceptor, R9, contributes a few additional microvilli (Fig. 3-1).

The spectral sensitivities of the photoreceptors are principally determined by their visual pigments, but may be modified by additional optical effects. Notably, clusters of pigment granules that are concentrated near the light-guiding rhabdoms act as long-pass filters and thus can shift the spectral sensitivity of the photoreceptors. Detailed studies on the small white butterfly, *Pieris rapae* (Pieridae), identified clusters of pale red and deep red pigments located inside the photoreceptors, adjacent to the rhabdoms. These pigments cause a pronounced shift towards red in the spectral sensitivity of the proximal photoreceptors. Whereas all proximal photoreceptors express a visual pigment with an absorption spectrum peaking in the green range at around 560 nm, photoreceptors in ommatidia with pale-red pigment have a spectral sensitivity peaking at 620 nm, and those in ommatidia with deep-red pigment have a peak sensitivity of 640 nm (Qiu and Arikawa 2003b; Wakakuwa et al. 2004). The receptors are accordingly termed red (R) and deep-red (dR) receptors.

When observed with an epi-illumination microscope, the eyes of most butterflies (with the exception of all papilionids and some pierids) exhibit a striking eyeshine, due to the presence of a tracheal tapetum at the bottom of the rhabdom (Fig. 3-1) (Bernard and Miller 1970; Arikawa and Stavenga 1997; Takemura et al. 2007). The tapetum reflects light that has escaped absorption while propagating through the rhabdom. Some of the reflected light travels back through the rhabdom and leaves the eye, and is visible as the eyeshine. The eyeshine spectrum (that is, the reflectance spectrum of the individual ommatidium) depends on the absorption by the visual pigments as well as the spectral filtering by the pigment clusters surrounding the rhabdoms, and thus the eyeshine color is a useful indicator of the type of ommatidium. In *Pieris rapae*, the individual ommatidia have eyeshine peaking at 635 nm or 675 nm. By a combination of histological, optical and electrophysiological methods, it could be demonstrated that ommatidia with reflectance spectra peaking at 635 nm contained 620 nm-peaking R-receptors and ommatidia with eyeshine peaking at 675 nm contained 640 nm-peaking dR-receptors (Qiu and Arikawa 2003b).

In the Pale Clouded Yellow butterfly, *Colias erate* (Pieridae), I have recently found that the eyeshine spectrum peaks near the infrared, at 730 nm, in a subset of ommatidia, suggesting that their photoreceptors may have a spectral sensitivity peaking at an even longer wavelength than those of *Pieris*. I therefore decided to perform an extensive study of the *Colias* eye, involving anatomical (Arikawa et al. 2009), molecular biological (Awata et al. 2009) and physiological (Pirih et al. 2010) analyses. I previously investigated the distal photoreceptors and found a clear sexual dimorphism due to sex-specific pigmentation of the ommatidia (Ogawa et al. 2012). Here I report a subsequent study on the properties of the proximal photoreceptors, with particular reference to the sexual dimorphism in their spectral sensitivities. I discovered that the long-wavelength receptors peaking in the wavelength range longer than 600 nm, which are generically called "red" receptors, are much more variable in females than in males, implying that females have an improved wavelength discrimination ability in the long wavelength region of the spectrum.

Material and methods

Animals

Adults of the Eastern Pale Clouded Yellow butterfly, *Colias erate* Esper, were obtained from a laboratory culture derived from eggs laid by females captured around the Sokendai-Hayama campus, Kanagawa, Japan. Hatched larvae were reared under natural light conditions on fresh clover leaves.

Electrophysiology and dye injection

Electrophysiological methods were as described previously (Ogawa et al. 2012). Briefly, photoreceptor spectral sensitivities were determined by intracellular recording of responses to monochromatic stimuli delivered by a 500 W Xenon arc lamp via a series of narrow-band interference filters ranging from 300 to 740 nm. The light beam was focused on the tip of an optical fiber, the other end of which was attached to a Cardan-arm perimeter device in a Faraday cage, where it provided a point light source (1° in diameter). The quantum flux of each monochromatic stimulus was measured using a radiometer (Model-470D, Sanso, Tokyo, Japan) and adjusted to a standard number of photons using an optical wedge. For each experiment, a butterfly was mounted on a plastic stage in the Faraday cage, with its dorsal side up. A silver wire inserted into the head served as the reference electrode. A glass microelectrode filled with 10 mM Alexafluor 568 (peak excitation/emission at 576/599 nm) in 200 mM KCl (A10441, Molecular Probes, USA), with a resistance of about 100 MΩ, was inserted into the retina through a small hole made in the cornea. Membrane potentials were recorded through a preamplifier (MEZ-7200; Nihon Kohden, Tokyo, Japan) connected to a computer via an AD converter (MP-150, BIOPAC Systems, USA).

After penetrating a photoreceptor, the optical fiber was adjusted so as to yield maximal responses. First, the spectral type of the impaled photoreceptor was determined using a series of monochromatic flashes of duration 30 ms, spaced 1 s apart. The response-stimulus intensity (V-log I) function was recorded over a 4 log unit intensity range at the photoreceptor's peak wavelength. The photoreceptor was subjected to further analyses only if the maximal response amplitude exceeded 30 mV. At the end of the recording, Alexafluor 568 was injected into the photoreceptor by applying a 2 nA hyperpolarizing DC current for approximately 5 min.

Anatomy

Immediately after the electrophysiological experiment, I observed the eyes with a fluorescence microscope (Olympus, BX50) applying 550 nm excitation light, and thus localized and

photographed the ommatidium containing the dye-filled photoreceptor. I fixed the eyes in 4 % paraformaldehyde in 0.1 mol sodium cacodylate buffer (pH 7.4) at room temperature for 30 min, then embedded the eyes in Quetol 812 (Nisshin EM, Tokyo, Japan) and made a series of 10 μm-thick transverse sections. Subsequently I identified the type of the ommatidium containing the dye-filled photoreceptor based on the pigmentation pattern (as revealed by normal transmitted light microscopy) combined with the fluorescence and eyeshine pattern of the intact eye. To determine the distribution of the perirhabdomal pigment along the rhabdom, I fixed intact eyes as described above and cut 5 μm-thick serial sections from the distal to the proximal end of the rhabdom.

Microspectrophotometry

The absorbance spectra of the perirhabdomal pigments were measured from pigment clusters in transverse light-microscopic sections using a microspectrophotometer consisting of a Leitz Ortholux microscope, with an Olympus 20x objective (NA 0.46), connected to an Avaspec 2048-2 CCD detector array spectrometer (Avantes, Eerbeek, Netherlands).

Model calculation

To quantitatively estimate the spectral sensitivity of the proximal photoreceptors of *Colias erate*, I constructed an optical simulation model based on the anatomical details of the three types of ommatidia (I, II and III) present in the eye of *Colias* (Arikawa et al. 2009). Based on the anatomical study of Arikawa et al. (2009), we used the following values in the model calculations. The total length of the rhabdom was 500 μm (Fig. 3-2). The depth of the upper tier of the rhabdom, with rhabdomeres of photoreceptors R1-4, was 250 μm in type I ommatidia, and 200 μm in type II and III ommatidia. The depth of the second tier (containing the rhabdomeres of photoreceptors R5-8) was the remaining part of the rhabdom, except for the basal 10 μm, which was assumed to be fully occupied by the rhabdomere of R9. A fluorescent pigment, whose absorbance spectrum was assumed to be identical to that of the fluorescent pigment in *Pieris rapae* (Arikawa et al. 2005), was present in the most distal 80 μm of the rhabdoms in type I ommatidia in male eyes and in type II ommatidia of female eyes (Ogawa et al. 2012). The visual pigment expressed in each photoreceptor (Awata et al., 2009; Ogawa et al., 2012) and the occupancy ratio of the rhabdomeres in the entire rhabdom (Arikawa et al., 2009) are shown in Table 3-1.Visual pigment absorbance spectra were calculated using the Govardovskii template (Govardovskii et al. 2000). I applied the simple model approach of Stavenga and Arikawa (2011) and thus ignored the wave-optical properties of the dioptric system and rhabdom. The transmittance of a rhabdom layer with thickness Δz is given by

$$T(\lambda) = \exp\left[-\kappa(\lambda)\Delta z\right] \tag{1}$$

with

$$\kappa(\lambda) = \kappa_{\mathrm{V}}(\lambda) + \kappa_{\mathrm{S}}(\lambda) \tag{2}$$

where $\varkappa_{\mathrm{V}}$ is the local absorbance coefficient due to absorption by the visual pigments, which is given by

$$\kappa_{\mathrm{V}} = \kappa_{\mathrm{V,max}} \left\{ \sum \alpha_i(\lambda) \rho_i \right\} \tag{3}$$

where $\varkappa_{\mathrm{V,max}}$ is the peak absorbance coefficient, α_i is the normalized absorbance spectrum of the visual pigment in photoreceptor Ri (i = 1-8), and ϱ_i is the occupancy ratio of the rhabdomere of photoreceptor Ri in the rhabdom. $\varkappa_{\mathrm{S}}$ represents the absorbance coefficient of the fluorescent pigment as well as the perirhabdomal pigment,

$$\kappa_{\mathrm{S}} = \kappa_{\mathrm{S,max}} \alpha_{\mathrm{S}}(\lambda) \tag{4}$$

with $\varkappa_{\mathrm{S,max}}$ the peak absorbance coefficient and α_{S} the normalized absorbance spectrum. The light flux at location z, $I(z,\lambda)$, is reduced into that at location $z + \Delta z$, $I(z + \Delta z)$, by

$$I(z + \Delta z, \lambda) = T(\lambda) I(z, \lambda) \tag{5}$$

The light flux absorbed by the visual pigment of the individual photoreceptors in a compartment of depth Δz is given by

$$\Delta A_i(\lambda) = \left[I(z,\lambda) - I(z + \Delta z, \lambda) \right] \kappa_{\mathrm{V,max}} \alpha_i(\lambda) \rho_i / \kappa(\lambda) \tag{6}$$

I assumed that at all wavelengths a unit light flux entered the ommatidia. Before reaching the photoreceptors, the incident light first passes the dioptric apparatus, consisting of the corneal facet lens and crystalline cone. I assumed that the transmittance of the dioptric apparatus was equivalent to that of the moth *Endromis* (Bernhard et al. 1965). Its transmittance spectrum, $T_C(\lambda)$, is thus identical to the relative light flux spectrum $I_0(\lambda)$ at z = 0 μm, the tip of the rhabdom. Summing the absorbed light fractions of the individual photoreceptors over the different rhabdom compartments then yields the photoreceptor's absorbance spectrum. Normalizing this yields the spectral sensitivity.

Calculation of wavelength discrimination (DI) function

I have calculated the wavelength discrimination of the visual system of *Colias erate* with a receptor noise-limited color opponent model (Vorobyev and Osorio 1998). This model is based on two assumptions that visual thresholds are set by noise originating in the photoreceptors and that achromatic (intensity-based) cues are not used for color discrimination. The model estimates a perceptual distance between two stimuli, ΔS. When ΔS is below threshold, two stimuli differing $\Delta\lambda$ in wavelength cannot be discriminated. This condition allows me to calculate $\Delta\lambda$ as a function of

wavelength. Without loss of generality, the threshold distance can be assumed to be equal 1: in this case, the perceptual distance is measured in terms of the just noticeable distance. In the case of vision based on *n* classes of photoreceptors, the distance between stimuli is given as follows:

$$(\Delta S)^2 = \frac{\sum_{1\le i<j\le n}^{n}\left(\Delta f_i - \Delta f_j\right)^2/\left(\omega_i \omega_j\right)^2}{\sum_{i=1}^{n} 1/{\omega_i}^2} \tag{7}$$

where Δf_i is the difference between the signals of a photoreceptor *i* and ω_i is the noise of receptor mechanism *i*. To describe the receptor signal f_i for stimuli that differ significantly from the adapting light, which is background light i.e. to the room illumination, I used a logarithmic relationship between the receptor quantum catches q_i and the receptor signals. The logarithmic model is a mathematical formulation of Weber's law, and for this model ω_i is equivalent to the Weber fraction of receptor mechanism *i*. The logarithmic model predicts that for any two stimuli ΔS does not depend on the intensity of these stimuli. However, the logarithmic model has an obvious limitation – it cannot be used for stimuli producing a zero quantum catch in one of the photoreceptors, because a logarithm of 0 is equal to negative intensity. To overcome this limitation, I assume that the f_i are given as follows:

$$f_i = \ln(1 + q_i)\ \mathrm{f_i} = \ln(1 + \mathrm{q_i}) \tag{8}$$

where ln is the natural logarithm and q_i is the normalized quantum catch of a photoreceptor *i*. Because the receptor noise-limited color opponent model assumes that signals that differ only in intensity from the background produce a zero color opponent signal, receptor sensitivities must be normalizes to background light. For monochromatic light of wavelength λ and intensity I_0 , the quantum catches are given as follows:

$$q_i(\lambda) = I_0 k_i P_i(\lambda), \tag{9}$$

where $P_i(\lambda)$ is the spectral sensitivity of photoreceptor *i* and $k_i = c \,/\, \int P_i(\lambda)\, I(\lambda)\mathrm{d}\lambda$. Here, $I(\lambda)$ is the light intensity distribution as a fraction of wavelength λ, and parameter *c* is chosen so that the *k* value for R (red) receptors k_R equal 1. I further assume that the intensity of the monochromatic stimuli I_0 is equal to 1, which implies that lights are not discriminated on the basis of intensity differences.

Because the threshold distance is set to 1, the minimum discriminable wavelength difference Δλ can be found from the condition

$$\Delta S(\Delta\lambda) = 1. \tag{10}$$

For small Δλ

$$\Delta f_i = \frac{df_i}{d\lambda}\Delta\lambda. \tag{11}$$

Substitution of equations (10) and (11) into equation (7) gives the minimum discriminable

wavelength difference

$$\Delta\lambda = \sqrt{\frac{\sum_{i=1}^{n} 1/{\omega_i}^2}{\sum_{1\le i<j\le n}\left(\frac{df_i}{d\lambda}-\frac{df_j}{d\lambda}\right)^2/\left(\omega_i\omega_j\right)^2}} \quad (12)$$

$$\frac{df_i}{d\lambda} = \frac{k_i}{1+k_iP_i}\frac{dP_i}{d\lambda} \quad (13)$$

To calculate the derivatives of the photoreceptor spectral sensitivities $P_i(\lambda)$, the sensitivities were approximated as sum of three Gaussian functions

$$P_i(\lambda) = A_i\exp\left(-\frac{\left(\lambda-\lambda_i^0\right)^2}{2\delta_i^2}\right) + B_i\exp\left(-\frac{\left(\lambda-\lambda_i^1\right)^2}{2\sigma_i^2}\right) + C_i\exp\left(-\frac{\left(\lambda-\lambda_i^2\right)^2}{2\rho_i^2}\right) \quad (14)$$

Where A_i, B_i, C_i, λ_i^0, δ_i, λ_i^1, σ_i, λ_i^2, ϱ_i are parameters whose values were adjusted to provide approximation of measured spectral sensitivities.

To estimate ω_i, I used a method previously applied to model the behavioral spectral sensitivity of some animals (Vorobyev and Osorio 1998). Because the signal-to-noise ratio can be improved by the summation of signals of individual photoreceptors, the relative noise level is inversely proportional to the number photoreceptors of a given spectral type $\omega_i = \nu_i / \sqrt{\eta_i}$, where ν_i is the noise level of a single photoreceptor and η_i is the number of receptors of a type i. I assume that different cells have similar levels of noise and set the noise of the R receptor to 0.05, i.e.

$$\omega_i = 0.05\sqrt{\frac{\eta_R}{\eta_i}} \quad (15)$$

The choice of the noise value for the R receptor to be 0.05 does not follow from actual measurements, but it is a value used in previous theoretical studies of animal vision (Vorobyev 2003; Schaefer et al. 2007).

Results

Sexually dimorphic perirhabdomal pigment

The ommatidia of *Colias* can be divided into three types, I-III, according to their characteristic patterns of perirhabdomal pigmentation (Fig. 3-3). In a previous study on male *Colias* (Arikawa et al. 2009), I reported that the perirhabdomal pigments of all three ommatidial types have the same red color (Fig. 3-3a). However, further anatomical studies revealed that in the female the pigment in type II ommatidia is orange (Fig. 3-3b).

I measured the absorbance spectra of the perirhabdomal pigments by microspectrophotometry. The absorbance spectra of the red pigment clusters of males and females were virtually identical, but the spectrum of the orange pigment in female type II ommatidia was different (Fig. 3-3c). Because the microspectrophotometer did not allow reliable measurements in the ultraviolet range, the spectra were assumed to be constant below 366 nm: in fact the absorbance of the pigments in the UV wavelength region had negligible effect on the sensitivity of the red receptors. The mean spectra of Fig. 3-3c were used in the model calculations.

The perirhabdomal pigments are located near the rhabdom in the soma of the proximal photoreceptors, R5-8. To investigate the distribution of the pigments along the rhabdom, I examined a series of 5 μm-thick plastic sections of eyes of both sexes. The pigmented regions differed between the ommatidial types (Fig. 3-2). The orange pigmented region of the female type II ommatidia is shorter (150 μm) than the region of the red pigment in the other ommatidial types (230 μm), indicating weaker filtering by the orange pigment. In both sexes, the pigment in type I ommatidia extends slightly deeper than in type II and III ommatidia (Fig. 3-2).

Spectral sensitivities of proximal photoreceptors

I measured the spectral sensitivities of the proximal photoreceptors, R5-8, in all three types of ommatidia in the ventral region of both male and female eyes. Of the more than 100 recordings, 28 photoreceptors were successfully labeled and thus analyzed in detail. Figure 3-4 shows examples of labeled photoreceptors from each ommatidial type of each sex. For each of the photoreceptors, the top, middle and bottom panels respectively show the spectral sensitivity, the ommatidial array as observed with regular transmission light microscopy, and the array as observed with fluorescence microscopy revealing the Alexafluor-filled photoreceptor cell body.

All photoreceptors in Fig. 3-4 are maximally sensitive in the wavelength region above 600 nm and are therefore collectively called “red” receptors. However, the spectral sensitivity

profiles in the different ommatidial types differ from each other in both sexes. For example, in type I ommatidia, the male R5 photoreceptor (Fig. 3-4a) has its main peak at 680 nm and a large secondary peak at 480 nm, while the female R5 (Fig. 3-4d) exhibits a single peak at 640 nm. Similarly, a large secondary sensitivity exists in type II ommatidia only in males (Fig. 3-4b, e).

The spectral sensitivities of individual photoreceptors differ slightly even within one ommatidial type and sex (Fig. 3-4). The mean spectral sensitivities of R5-8 in males peak at 660-680 nm in all ommatidial types. In females, the mean spectral sensitivities peak at 640-660 nm in type I, 600-620 nm in type II and 660-680 nm in type III ommatidia (Fig. 3-5). I shall distinguish these red (R) receptors by adding their sex, male (m) or female (f), and the ommatidial type, I, II, or III; e.g., RmI indicates a red receptor in type I ommatidia of males and RfII is a red receptor in type II ommatidia of females (Fig. 3-5).

Model calculations

Figure 3-5 shows averaged spectral sensitivities of the various classes of red receptors, which were localized by dye injection and identified by anatomy. We use the averaged spectral sensitivities as the representatives of the red receptors of the different ommatidial types.

In my previous paper on the distal R1-4 photoreceptors of *Colias*, I could quantitatively describe the measured spectral sensitivities with a simple (heuristic) model of the distal rhabdom tier (Ogawa et al. 2012). I extended this model by including the proximal tier in order to quantitatively estimate the spectral sensitivity of R5-8 photoreceptors. Figure 3-5 shows the means of the spectral sensitivities (symbols) measured in the photoreceptors of the different ommatidial types of male and female together with calculated spectra (continuous curves) obtained by using the following parameter values. All visual pigments had a peak absorbance coefficient $\varkappa_{V,max} = 0.005\ \mu m^{-1}$. The peak absorbance coefficient of the fluorescent pigment in male type I and female type II ommatidia was $\varkappa_{S,max} = 0.02\ \mu m^{-1}$. The peak absorbance coefficient of the perirhabdomal pigment, with absorbance spectra given by Fig. 3-3c, was $\varkappa_{S,max} = 0.03\ \mu m^{-1}$ (for both the red and orange pigment); the longitudinal density distribution as shown in Fig. 3-2 was assumed to be constant. The visual pigment CeL (Awata et al. 2009), expressed in all proximal photoreceptors, was R565, i.e., its peak absorption was at 565 nm (Ogawa et al. 2012). Modifying the assumed parameter values in a realistic range did not essentially change the results.

The model successfully reproduced the profile of the main sensitivity band of all proximal photoreceptors. In males, the peak wavelength of the calculated spectra is 660 nm in all ommatidial types (Fig. 3-5a-c). In females, it is 650 nm in type I (Fig. 3-5d), 610 nm in type II (Fig.

3-5e) and 660 nm in type III (Fig. 3-5f). Although male and female type I ommatidia have the same red pigment and rhabdoms of similar dimensions, the spectral sensitivities of the proximal photoreceptors differ due to a difference in length of the pigmented region, which is about 35 μm shorter in females (Fig. 3-2). The present model did not reproduce the secondary sensitivity bands in the short wavelength region showing that the model is incomplete as will be discussed below.

Wavelength discrimination

To investigate this wavelength discrimination ability, I have applied the receptor noise-limited color opponent model (Vorobyev and Osorio 1998) to the *Colias* visual system (Fig. 3-7a). For comparison, I performed the same analysis for the visual system of *Pieris rapae* (Fig. 3-7b). I assumed that all spectral receptors of an eye participate in the wavelength discrimination system. The number of photoreceptors of each type is based on the actual distribution of receptors in the eye shown in Table 3-2. To provide approximation of measured spectral sensitivities, parameters (A_i, B_i, C_i, λ_i^0, δ_i, λ_i^1, σ_i, λ_i^2, ϱ_i) were adjusted. The values and resulting spectra are shown in Table 3-3 and Fig. 3-8.

The wavelength discrimination ability is limited around 650 nm in *Colias* males (Fig. 3-7a, blue line). In contrast, *Colias* females extend their discriminable range to much longer wavelengths up to about 700 nm (Fig. 3-7a, red line). Both male and female *Pieris rapae* have the wavelength discrimination in the red wavelength range is similar, extending to about 670 nm (Fig. 3-7b).

Discussion

Red receptors in Colias erate

I characterized the spectral sensitivities of the proximal photoreceptors in the compound eye of *Colias erate* by intracellular recording and optical modeling. All photoreceptors were maximally sensitive in the red wavelength region, but their peak wavelengths differed strikingly between males and females. According to the actual recordings and model calculations, I conclude that the proximal photoreceptors of males peak at 660 nm in all ommatidial types, and those in females peak at 610, 650 or 660 nm depending on the ommatidial type. To the best of my knowledge, 660 nm is the longest peak wavelength of any red receptor reported in an insect. This is also the first example of a distinct sexual dimorphism of red receptors in any animal.

The simple model I applied could well reproduce the principal sensitivity peaks of the red receptors. Two mechanisms appeared to account for the differences in the calculated sensitivity spectra. First, the different absorbance spectra of the red and orange pigment clusters mean that different spectral filters act on the proximal photoreceptors (Fig. 3-2, 3). Second, the orange pigment in the female type II ommatidia extends over just 150 μm (Fig. 3-2), which is much shorter than in the other ommatidia, resulting in a lower density of the pigment filter. Accordingly, the proximal photoreceptors in female type II ommatidia have the shortest peak wavelength (620 nm). Furthermore, the extent of red pigment in type I ommatidia is longer in males (265 μm) than that in females (230 μm). Consequently, the spectral sensitivity of the proximal photoreceptors in type I ommatidia peaks at 660 nm in the male and at 640 nm in the female.

The modeled spectra deviate markedly from the experimental spectra in the short- and middle-wavelength range, where the calculations predict a low sensitivity but the measured spectra show distinct sensitivity bands (Fig. 3-5). The same problem was encountered in the study of the small white butterfly, *Pieris rapae*. In that instance, calculations with a similar simple model also yielded low sensitivities in the short and middle wavelength range. An elaborate wave-optical model of the *Pieris* rhabdom produced substantial sensitivity bands in the shorter wavelength range (Stavenga and Arikawa 2011). My attempts to construct a wave-optical model similar to that of *Pieris* have remained somewhat unsatisfactory, due to the considerably more complicated structure of the rhabdoms of *Colias*; whereas the rhabdoms of *Pieris* approximate a homogeneously tapering cylinder, the rhabdoms of *Colias* have a pronounced constriction in the middle (Arikawa et al. 2009). At the constriction, the rhabdomeric microvilli are locally replaced by concentrated red pigment. This makes wave-optical modeling difficult, because the rhabdoms' waveguide properties strongly

depend on both the rhabdom diameter and the refractive indices of the medium within and surrounding the rhabdom, which is unknown in the case of the red pigment. Nevertheless, preliminary modeling attempts yielded clear sensitivity bands in the short and middle wavelength range. From this observation, together with the exemplary case of *Pieris,* it seems reasonable to hypothesize that the ultraviolet and blue sensitivity bands of the proximal photoreceptors of *Colias* (Fig. 3-5) are due to waveguide effects.

Note that the RmI and RfI are similar in the principal peaks in red wavelength region, but the secondary sensitivity band in the UV-V wavelength region is smaller in RmI than in RfI (Fig. 3-5a, d). In type II red receptors, the relationship is reverse. This sexual difference is attributable, at least in part, to the sexually dimorphic distribution of the fluorescence filter pigment (Fig. 3-3c): the male type I and the female type II ommatidia contain the fluorescence pigment (Ogawa et al. 2012).

Function of the multiple red receptors

Remarkably, the expression pattern of visual pigments is identical in both sexes of *Colias erate* (Awata et al. 2009; Ogawa et al. 2012), but the spectral sensitivities of their photoreceptor sets differ. Sexual dimorphism in photoreceptor spectral sensitivities was already encountered in the distal photoreceptors of *Colias* (Ogawa et al. 2012). A fluorescent pigment that absorbs maximally at around 420nm, concentrated near the distal tip of the rhadbom in male type I ommatidia and female type II ommatidia, produces shouldered-blue receptors (sB) in males and narrow-blue receptors (nB) in females (Fig. 3-6, see also Chapter 2). Together with the present study, this shows that the sexual dimorphism of *Colias* eyes is rather pronounced (Fig. 3-6, Table. 3-4). It is therefore most likely that males and females view the colored world quite differently. The eyes' set of spectral photoreceptors provides an animal with the ability to see color and/or to discriminate light sources that differ in wavelength. Extensive studies of wavelength discrimination in the honeybee *Apis mellifera* (von Helversen 1972) demonstrated that the threshold for wavelength discrimination (that is, the minimal discriminable wavelength difference) is the lowest at wavelengths in between the sensitivity peaks of the trichromatic set of photoreceptors (Kelber et al. 2003). The eye of the Japanese yellow swallowtail butterfly, *Papilio xuthus*, has eight classes of photoreceptor, distributed in three types of ommatidia. Behavioral tests revealed that the wavelength discrimination acuity of *Papilio* butterflies is maximal at 420, 480 and 560 nm. Assuming a spectral opponency mechanism between the spectral receptors through the interphotoreceptor connections in the lamina (Takemura and Arikawa 2006), we applied the receptor noise-limited color opponent model (Vorobyev and Osorio 1998) to identify the photoreceptors that were involved in the wavelength discrimination behavior in *Papilio*.

Thus, it was suggested that only four spectral classes of photoreceptors participate in wavelength discrimination, i.e. *Papilio* is tetrachromatic (Koshitaka et al. 2008).

The sexual dimorphism of the spectral photoreceptors of *Colias* implies that wavelength discrimination differs between the two sexes. As expected, wavelengths above around 650 nm cannot be distinguished by *Colias* males, due to the sensitivities of all red receptors peak at 660 nm (Fig. 3-7a, blue line). In contrast, *Colias* females have a set of three red receptors, which extends their discriminable range to much longer wavelengths up to about 700 nm (Fig. 3-7a, red line). Both male and female *Pieris rapae* have the same two types of red receptor, R (620 nm) and dR (640 nm) (Qiu and Arikawa 2003b). In both sexes wavelength discrimination in the red wavelength range is similar, extending to about 670 nm (Fig. 3-7b). Clearly, *Colias* females should have the best spectral resolution in the longer wavelength range.

Red receptors are presumably crucial for female lycaenids to identify larval food sources (Bernard and Remington 1991). Similarly, the ovipositing Australian orchard butterfly *Papilio aegeus* uses a red receptor peaking at 610 nm to select young green leaves as being the best food for larvae (Kelber 1999a). These examples suggest the hypothesis that the three red receptors of *Colias* females are highly beneficial for detecting suitable leaves for oviposition. The light reflected by leaves is highest in the green and red ranges, but weaker additional reflections occur at shorter wavelengths. The sensitivity bands of the photoreceptors in the short- and middle-wavelength ranges (Fig. 3-5) will hence create a non-negligible background signal, but the high red sensitivity – especially the strongly red-shifted spectral sensitivity of the proximal photoreceptors in female type III ommatidia – will enable the discrimination of subtle differences in leaf coloration. Some of the spectral receptors of *Colias* have high polarization sensitivity as well (Pirih et al. 2010), which might enhance the spectral discrimination as in the case of *Papilio* (Kelber 1999b). Of course, not all spectral receptors necessarily contribute to the wavelength discrimination process, as is exemplified by *Papilio xuthus* (Koshitaka et al. 2008). Elucidation of the actual wavelength discrimination ability of *Colias* will require behavioral experiments.

Regionalization and sexual dimorphism of the Colias erate retina

The eye of *Colias erate* has a clear discontinuity between the dorsal third and the ventral two-thirds (Awata et al. 2009). The dorsal region is characterized by its light pigmentation (Arikawa et al. 2009) and the absence of the blue-absorbing visual pigment CeB (Ogawa et al. 2012). I have performed some preliminary studies to investigate whether the dorsal photoreceptors are also sexually dimorphic. However, intracellular recordings did not reveal any sexual dimorphism in the

distal nor proximal tiers of the dorsal retina. The proximal photoreceptors in the dorsal region of both sexes were maximally sensitive at 600-620 nm, and the spectral sensitivity curves had no secondary peak sensitivities in the shorter wavelength range (c.f. Fig. 3-5e). This is presumably due to the low density of perirhabdomal pigments, resulting in only moderate filtering. The experimental results indicated that the dorsal eyes of both males and females have the same, rather simple set of UV, V, G and R receptors. Possibly, the visual system of the dorsal retina mediates general visual activities, such as flight control and evading predators. The ventral retina may have evolved to mediate sexual behaviors including courtship and oviposition.

Figures

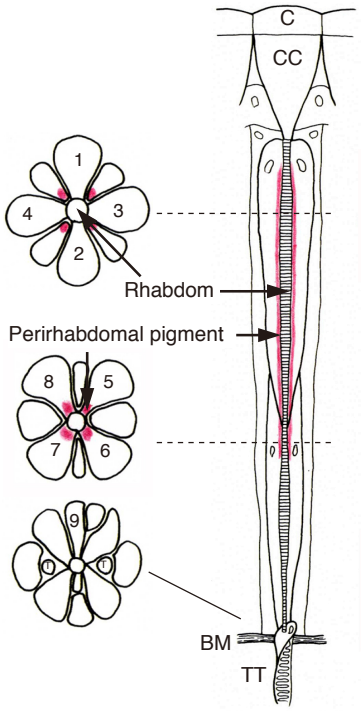

Fig. 3-1. Schematic diagram of a *Colias* ommatidium. Transverse views at three depths (left) at levels indicated in the longitudinal view (right). The numbers denote the nine photoreceptors, R1-9. The four distal photoreceptors, R1-4, contribute microvilli to the distal two-thirds of the rhabdom, while the proximal one-third is composed of four proximal photoreceptors, R5-8. The basal photoreceptor, R9, adds some microvilli at the basal end of the rhabdom. The rhabdom is surrounded by four clusters of perirhabdomal pigment, which are located in the cell bodies of the R5-8 photoreceptors; the cell bodies extend distally between the cell bodies of R1-4. C, cornea; CC, crystalline cone; BM, basement membrane; T, trachea; TT, tracheal tapetum.

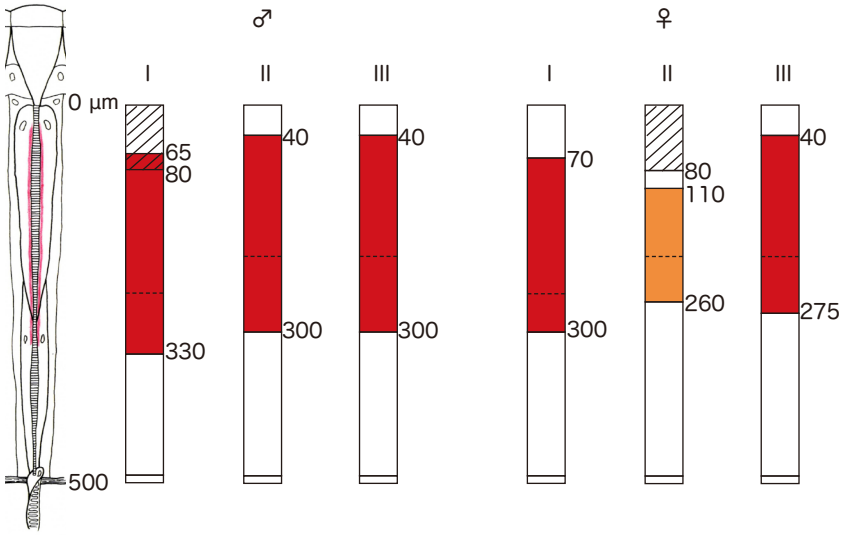

Fig. 3-2. Diagram of the dimensions assumed in the optical modeling of the rhabdom. Left: diagram of an ommatidium of *Colias erate*. Right: simple compartment models of the rhabdoms in ommatidial types I-III of male and female. The total length of each rhabdom was assumed to be 500 µm with the distal tier occupying 250 µm in type I ommatidia and 200 µm in type II and III ommatidia. The distribution pattern of the perirhabdomal pigments (red in all ommatidia except in the ommatidial type II of the female, see Fig. 3-3) depends on the type of ommatidium and the sex, as indicated. Diagonal lines show the location of fluorescent pigment, in the male ommatidial type I and the female type II.

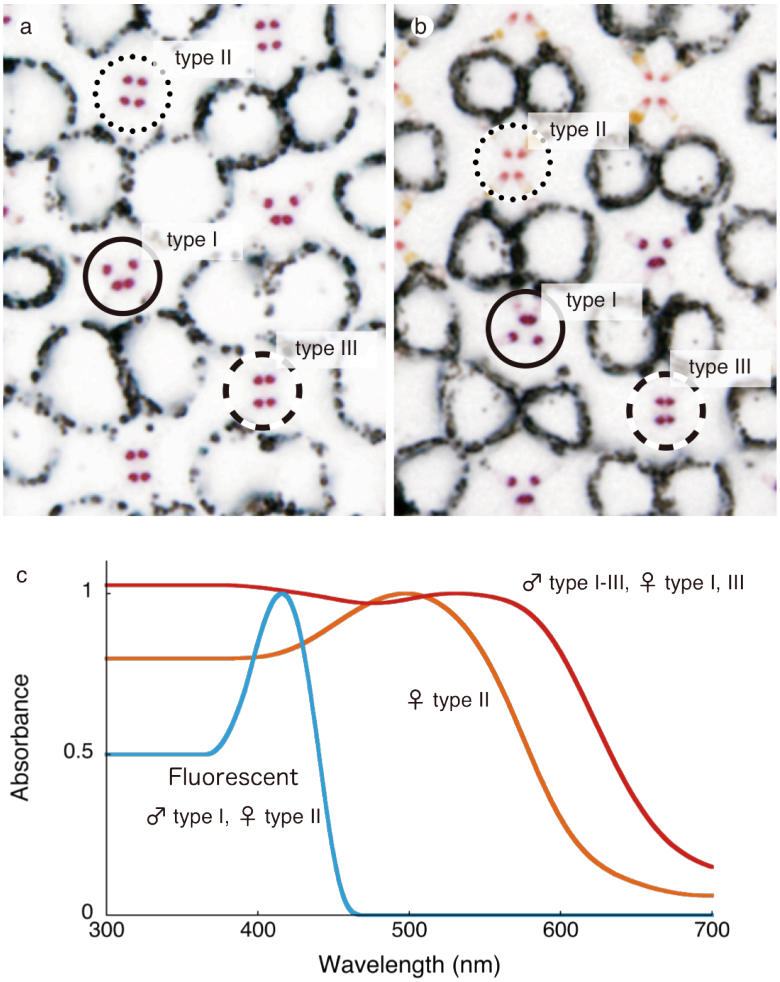

Fig. 3-3. Sexual dimorphism of the perirhabdomal pigments. (**a**) Light microscopic unstained plastic transverse section through the distal tier of the ventral part of the eye of a male *Colias* erate, showing pigment clusters arranged in trapezoidal (solid circle, type I ommatidium), square (dotted circle, type II), and hexagonal patterns (dashed circle, type III). In all three ommatidial types the pigment is red. (**b**) A similar section of the female ventral eye, showing the same three patterns of pigment clusters. However, the pigment in ommatidial type II is orange. (**c**) Averaged, normalized absorbance spectra of the red and orange perirhabdomal pigments, measured with a microspectrophotometer. Scale bar = 20µm.

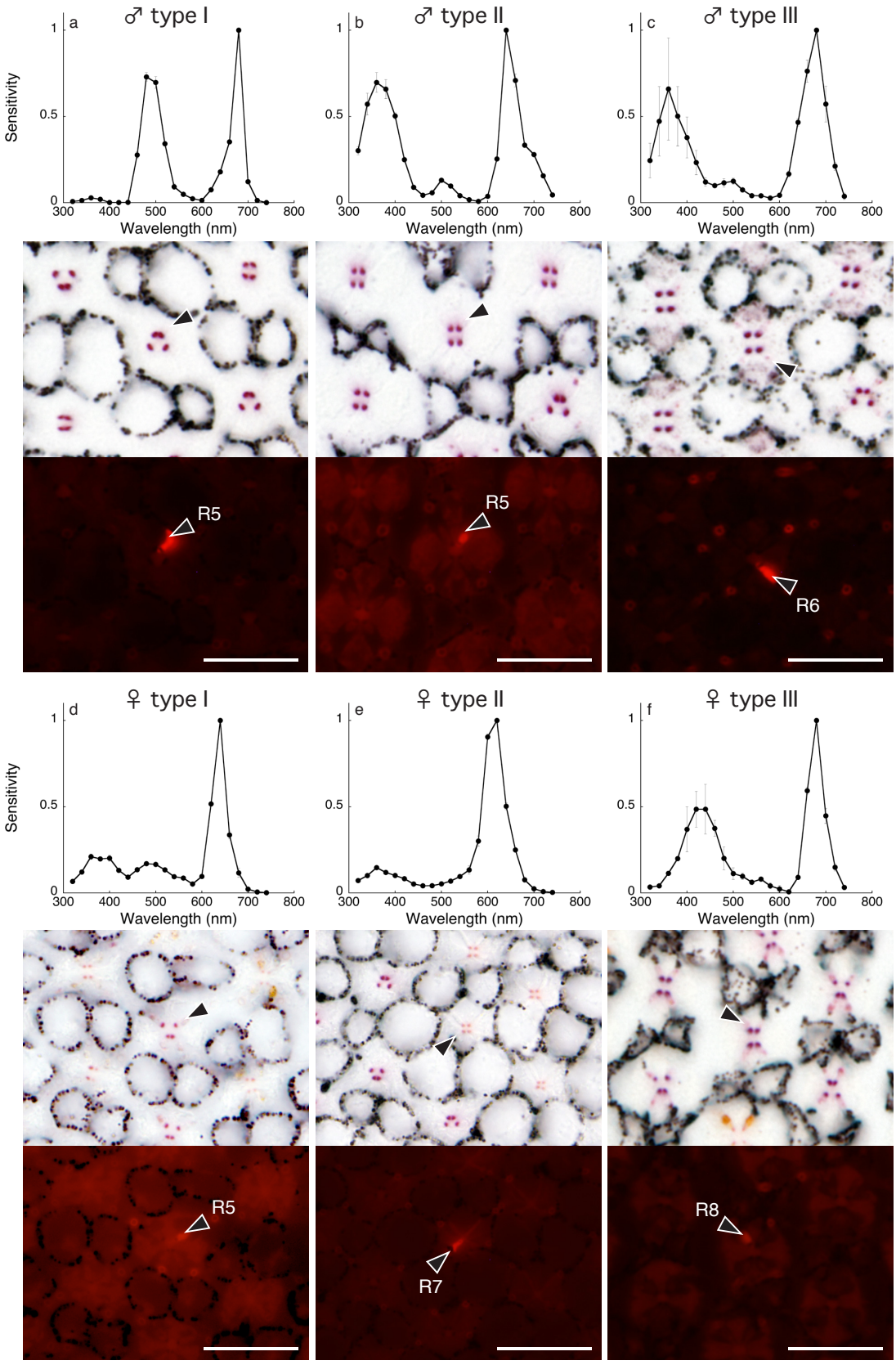
a
♂ type I
b
♂ type II
c
♂ type III
Sensitivity
Wavelength (nm)
R5
R5
R6
d
♀ type I
e
♀ type II
f
♀ type III
R5
R7
R8

Fig. 3-4. Six examples of proximal photoreceptors of *Colias erate*. Spectral sensitivity (top row); transmission light micrograph of the photoreceptor (arrowhead) in the ommatidial array (middle row) and its fluorescence image (bottom row, arrowhead). (**a**) Male R5 in a type I ommatidium. (**b**) Male R5 in a type II ommatidium. (**c**) Male R6 in a type III ommatidium. (**d**) Female R5 in a type I ommatidium. (**e**) Female R7 in a type II ommatidium. (**f**) Female R8 in a type III ommatidium. Scale bars: 20 μm.

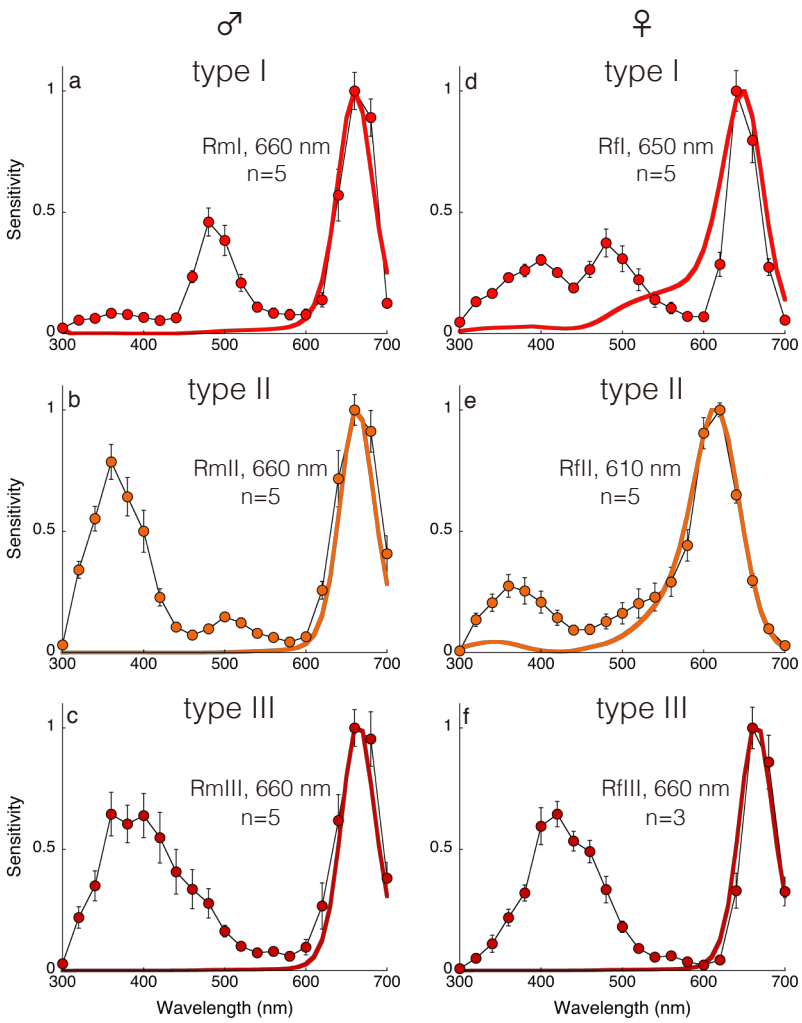

Fig. 3-5. Spectral sensitivities of proximal photoreceptors (mean ± standard error; n, sample number) with model calculations (colored curves). Each panel indicates the photoreceptor nomenclature, peak wavelength of the calculated spectrum and number of samples. (**a**) Mean spectral sensitivities of red receptors in male type I ommatidia, RmI. (**b**) Male type II, RmII. (**c**) Male type III, RmIII. (**d**) Female type I, RfI. (**e**) Female type II, RfII. (**f**) Female type III, RfIII.

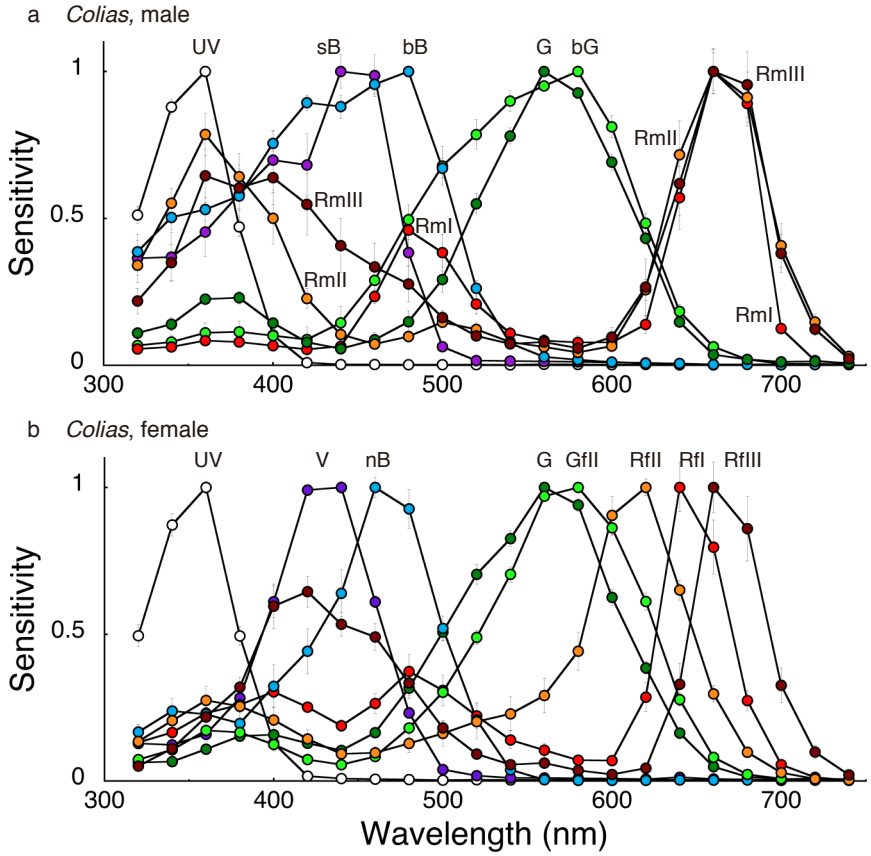

Fig. 3-6. Spectral sensitivities of all photoreceptor classes in males (**a**) and females (**b**) of *Colias erate*. The photoreceptors are divided into ultraviolet (UV), blue (V, nB, sB, bB), green (G, bG, GfII (green in female type II) and red (RmI, RmII, RmIII, RfI, RfII, RfIII) classes. The blue and red receptor classes are sexually dimorphic

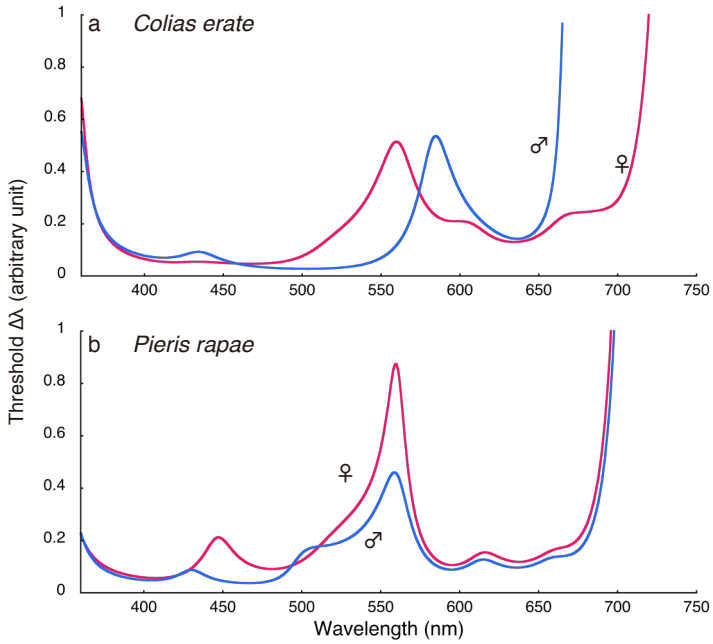

Fig. 3-7. Wavelength discrimination threshold (arbitrary units) predicted by a receptor noise-limited color opponent model. (**a**) Threshold for male and female *Colias erate* when all photoreceptors are assumed to participate. (**b**) Threshold for male and female *Pieris rapae*.

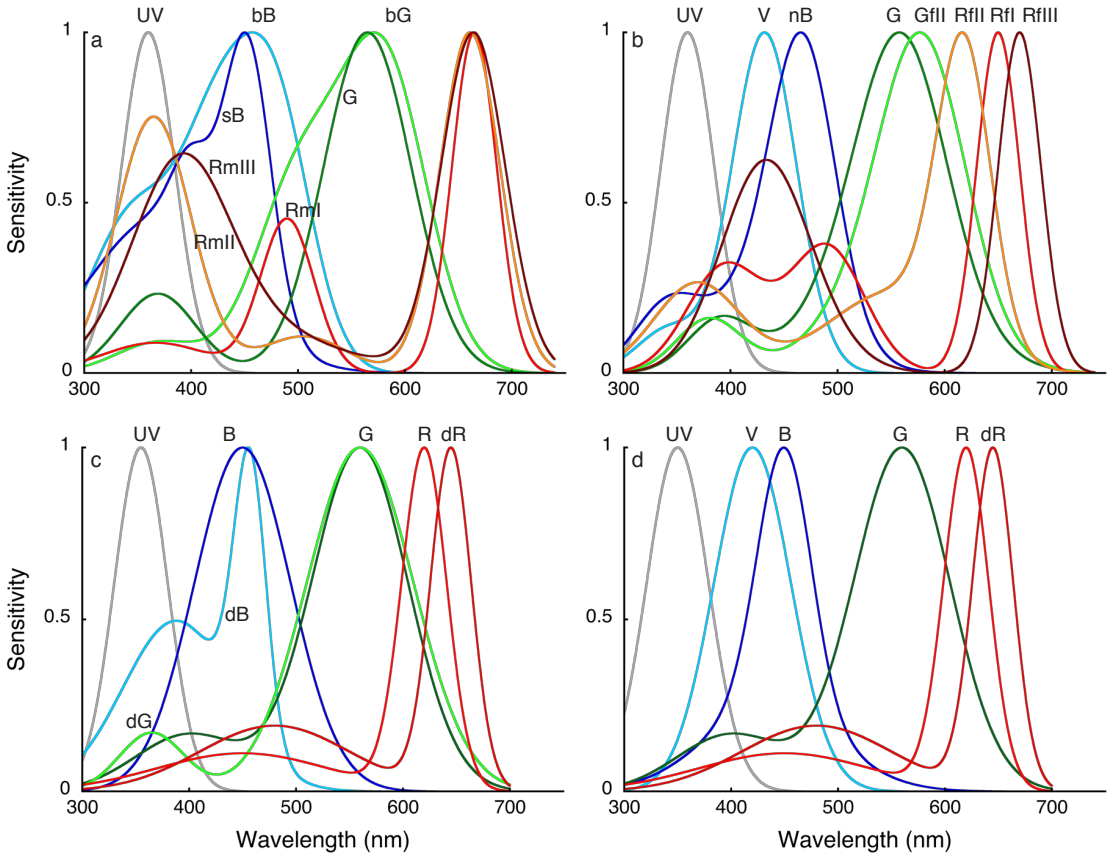

Fig. 3-8. Gaussian fits of photoreceptor spectral sensitivities, which were used for calculating D*l* function. (**a**) *Colias erate* male, (**b**) *Colias erate* female, (**c**) *Pieris rapae* male, (**d**) *Pieris rapae* female.

Table 3-1. Parameters used in the model

	$\kappa_{S,max}$		Visual pigment absorption peak / rhabdomere occupancy ratio			
	♂	♀	R1	R2	R3 & 4	R5-8
type I	3.0	2.5	360 nm / 0.40	430 nm / 0.40	565 nm / 0.15	565 nm / 0.25
type II	2.8	1.0	430 + 460 nm / 0.35	430 + 460 nm / 0.35	565 nm / 0.15	565 nm / 0.25
type III	3.0	4.0	360 nm / 0.35	360 nm / 0.35	565 nm / 0.15	565 nm / 0.25

$\kappa_{S,max}$; absorbance coefficient of red pigment

Table 3-2. The number of photoreceptors of each types

	Ratio	R1	R2	R3/4	R5-8
Colias erate male					
I	50%	UV	sB	bG	RmI
II	35%	bB		G	RmII
III	15%	UV		G	RmIII
Colias erate female					
I	50%	UV	V	G	RfI
II	35%	nB		IIG	RfII
III	15%	UV		G	RfIII
Pieris rapae male					
I	50%	UV	B	G	R
II	25%	dB		dG	DR
III	25%	UV		G	R
Pieris rapae female					
I	50%	UV	B	G	R
II	25%	V		G	DR
III	25%	UV		G	R

Table 3-3. Parameters used in equation (14) to approximate receptor spectral sensitivities

	A	λ^0	δ	B	λ^1	σ	C	λ^2	ϱ
Colias erate male									
UV	1	360	25	0	-	-	0	-	-
sB	1.1	480	33	1	425	35	0.7	345	40
dB	0.9	453	22	0.25	400	18	0.52	370	65
bG	1	580	40	0.1	370	40	0.6	500	40
G	0.88	565	41	0.205	369	35	0	-	-
RmI	0.89	665	21	0.4	490	25	0.079	367	50
RmII	0.93	661	28	0.1	505	40	0.7	365	35
RmIII	0.93	664	30	0.12	450	80	0.51	390	45
Colias erate female									
UV	1	360	25	0	0	0	0	-	-
V	1	432	30	0.13	343	30	0	-	-
nB	1	468	30	0.28	430	55	0.2	340	30
G	0.95	560	42	0.3	540	65	0.185	390	30
GfII	1	580	40	0.3	550	60	0.2	380	30
RfI	0.7	650	20	0.26	490	35	0.22	395	35
RfII	0.93	618	25	0.25	550	60	0.281	369	40
RfIII	0.93	670	20	0.5	430	40	0.1	460	45
Pieris rapae male									
UV	1	355	25	0	-	-	0	-	-
dB	0.73	457	15	0.45	388	50	0	-	-
B	1	450	45	0	-	-	0	-	-
G	0.9	560	45	0.15	400	50	0	-	-
dG	0.88	560	50	0.15	365	30	0	-	-
R	0.89	620	21	0.1	450	80	0	-	-
dR	0.93	645	19	0.18	480	70	0	-	-
Pieris rapae female									
UV	1	350	29	0	-	-	0	-	-
V	0.9	420	36	0	-	-	0	-	-
B	0.73	462.9	18.7	0.24	436.8	60.2	0	-	-
G	0.9	560	45	0.15	400	50	0	-	-
R	0.89	620	21	0.1	450	80	0	-	-
dR	0.93	645	19	0.18	480	70	0	-	-

Table 3-4. Three types of ommatidia of the *Colias erate* ventral eye

		Pigment	Fluorescence	Photoreceptor spectral sensitivity / opsin mRNA			
				R1	R2	R3/4	R5-8
type I	♂	Red	+	UV	sB	bG	RmI
	♀	Red	-	UV	V	G	RfI
				CeUV	*CeV1+V2*		*CeL*
type II	♂	Red	-	bB		G	RmII
	♀	Orange	+	nB		GfII	RfII
				CeV1+V2+B			*CeL*
type III	♂	Red	-	UV		G	RmIII
	♀	Red	-	UV		G	RfIII
				CeUV			*CeL*

Photoreceptor nomenclature: UV, ultraviolet; V, violet; sB, shouldered-blue; bB, broad-blue; G, green; bG, broad-green; GfII, green in female type II ommatidia, Rm(f)I(II,III), red of male (female) type I (II, III) ommatidia. See Fig. 3-6 for the spectral sensitivity curves. For opsins, see Awata et al., 2009; Chapter 2.

General Discussion and Conclusion

In this thesis, I described the physiological basis of color vision in the Eastern Pale Clouded yellow butterfly, *Colias erate* Esper, focusing on the production mechanism of the variety of spectral photoreceptors. I demonstrated that males and females of *Colias* have different set of eight classes of spectral photoreceptor in the ventral region of the eye. On the other hand, I could not detect any sexual dimorphism in the dorsal retina. The eight types of photoreceptor identified in the *Colias* ventral retina are generated by 1) duplication of opsin genes, 2) expression of multiple opsins in single photoreceptors and 3) the filtering effect of the fluorescent and perirhabdomal pigment. Together with previous studies, especially on the small white, *Pieris rapae*, and the Japanase yellow swallowtail *Papilio xuthus*, these mechanisms underlying various spectral receptors appear to be widespread among butterflies (Arikawa et al. 1987; Arikawa et al. 1999; Qiu and Arikawa 2003a, b; Arikawa et al. 2004; Arikawa et al. 2005).

Sexually dimorphic butterfly eyes have likely evolved independently multiple times through a variety of physiological mechanism. In the case of *Colias erate*, males and females have identical opsin expression pattern, but the sex-specific localization of fluorescent pigment and polymorphism of perirhabdomal pigment produce the sexually dimorphic spectral sensitivities of blue and red receptors, respectively. In *Pieris rapae*, there is no sexual difference in opsin expression pattern either, but the two blue receptors are different between sexes due to filtering effect of the male specific fluorescent pigment. The situation in Pieridae, however, differs completely from the case of the more recently evolved family of butterflies, Lycaenidae, in which *Lycaena rubidus* exhibits a sexually dimorphic distribution of visual pigments in the dorsal eye. The cost might be lower in changing the localization or distribution pattern of screening pigment compared to producing sex-specific opsin expression pattern in Pieridae.

Why and how does such sexual dimorphism of color vision system come into existence? An attractive hypothesis is related to the striking difference in wing colors between sexes. In *Pieris rapae*, it is indicated that female wing reflectance is more or less constant throughout the visible wavelength range, including UV, but male wing reflectance is minimal there (Arikawa et al. 2005). Presumably, the fluorescent pigment locating exclusively in male eyes has been recruited to improve spectral discrimination around 400 m, where male wing reflectance abruptly changes. In *Colias erate*, all males have yellow wings, whereas females are divided into two morphs, alba (whitish) and yellow. Lifetime mating frequency of the yellow morph was significantly lower than that of the alba morph (Nakanishi et al. 2000). This indicates that alba females are more attractive for males,

because white wings might be highly visible for males. Behavioral experiments are necessary to confirm this hypothesis in the future. No sexual dimorphism in the eye has been reported in the most ancestral butterfly family, Papilionidae. Their wings are generally similar between sexes, and therefore no sexual dimorphism possibly exists in the visual system. To reveal the relation sexual dimorphic eye to wings color difference, more comparative studies are needed focusing on sexual difference of screening pigments and opsin expression pattern in such as *Papilio memnon*, which has more obvious sexual difference in wings. If *Papilio memnon* would have sexual dimorphic eye, I would be able to state the relationship between sexual dimorphic wings color and visual system. If all member of Papilionidae would possess no sexual dimorphism in visual system, it would indicate that ancestral butterfly did not have sexual difference in vision, and obvious sexual difference in wings color and/or other factor co-evolved with visual system in evolutionary process.

Insects have long been thought to be red-blind due to the lack of red receptors in the eye of honeybee, the first species in which color vision was convincingly demonstrated. However, accumulated evidence by now suggests that many insect species including butterflies have red sensitive photoreceptors whose peak sensitivity exists in the wavelength region longer than 600 nm (Arikawa 2003; Qiu and Arikawa 2003b). It is also suggested that duplication of long wavelength opsins occurred several times independently in Papilionidae, Nymphalidae and Riodinidae, and one of them appears to have absorbance spectrum peaking at 600 nm in riodinids (Frentiu et al. 2007b). Here, I discovered red receptor having peak at 660 nm in *Colias erate*. The most conspicuous point is that the *Colias* females have three distinct types of red receptors each peaking at 610, 650 or 660 nm. To the best of my knowledge, 660 nm is the longest peak wavelength of any red receptor reported in an insect. This is also the first example of a distinct sexual dimorphism of red receptors in any animals. Thus, the visible wavelength range of butterflies with red receptor is extended probably beyond 700 nm, while the range is limited around 650 nm in most insects without red receptors.

Why do butterflies need to have the red receptor system? One possibility is the use of red flowers as food source. *Papilio* and *Pieris* can be trained to red flowers to take nectar from them, but the sexual dimorphism cannot be explained by this. The sexual dimorphism may be related for females to find quality host plants to lay eggs. *Colias* females lay eggs on clover leaves, which turn into yellow or red when they become old. The subtle difference in spectral reflectance from leaves might be a sensitive sign for the quality of leaves. Any behavioral experiments focusing this question would be particularly interesting.

Finally, I summarize the conclusion of this thesis.

Chapter 1

Microspectrophotometry with epi-illumination revealed all ommatidia have identical reflectance spectrum in dorsal region of the eye in both sexes. Although type I ommatidia reflect 660 nm and type II and III ommatidia reflect 730 nm in males, female type II ommatidia reflect throughout 620 to 730 nm but type I and III reflect 660 nm 730 nm as in male, respectively. Remarkable sexual difference of eyeshine spectrum in type II ommatidia results from female specific orange perirhabdomal pigment. Regionalization was also found by electroretinogram. Dorsal region of retina relatively sensitivities below 420 nm range, whereas ventral region sensitivities to 420 nm to 550 nm due to ommatidial distribution bias.

Chapter 2

I analyzed the visual pigments and spectral sensitivities of these distal photoreceptors in both sexes of *Colias erate*. Cells 1 and 2 (R1/2) in type II ommatidia express a newly discovered middle wavelength-absorbing opsin, CeB, in addition to two previously described middle wavelength-absorbing opsins, CeV1 and CeV2. This is the first example of three opsins co-expression in a single photoreceptor. Males and females have the same visual pigment expression patterns, but the photoreceptor spectral sensitivities are sexually dimorphic. The photoreceptors coexpressing three middle wavelength-absorbing opsins are broad-blue receptors in males, but in females they are narrow-blue receptors. Those with CeV1 and CeV2 are violet receptors in females, while they are shouldered-blue receptors in males. I found the sex-specific distribution of fluorescent pigment, which functions as a spectral filter and produces the sexual dimorphism in spectral sensitivity.

Chapter 3

I identified that perirhabdomal pigment color is red in all ommatidial types except for type II ommatidia of females, where the pigment is orange. Intracellular recordings demonstrated that the spectral sensitivities of the proximal photoreceptors (R5-8) of all ommatidia in both sexes are red receptors due to strongly tuning by the perirhabdomal pigments. According to the sex-specific pigments in type II ommatidia, the spectral sensitivities of the R5-8 photoreceptors of females peaked at 620 nm while those in males peaked at 660 nm. The measured spectral sensitivities could be well reproduced by an optical model assuming a long-wavelength-absorbing visual pigment with

peak absorbance at 565 nm. Whereas the sexual dimorphism was unequivocally demonstrated for the ventral eye region, dimorphism in the dorsal region was not found.

References

Applebury ML, Antoch MP, Baxter LC, Chun LL, Falk JD, Farhangfar F, Kage K, Krzystolik MG, Lyass LA, Robbins JT (2000) The murine cone photoreceptor: a single cone type expresses both S and M opsins with retinal spatial patterning. Neuron 27:513-523

Archer SN, Lythgoe JN (1990) The visual pigment basis for cone polymorphism in the guppy, *Poecilia reticulata*. Vision Res 30:225-233

Arikawa K (2003) Spectral organization of the eye of a butterfly, *Papilio*. J Comp Physiol A 189:791-800

Arikawa K, Inokuma K, Eguchi E (1987) Pentachromatic visual system in a butterfly. Naturwissenschaften 74:297-298

Arikawa K, Kinoshita M, Stavenga DG (2004) Color vision and retinal organization in butterflies. In: Prete FR (ed) Complex worlds from simpler nervous system. The MIT Press, Cambridge, London, pp 193-219

Arikawa K, Mizuno S, Kinoshita M, Stavenga DG (2003) Coexpression of two visual pigments in a photoreceptor causes an abnormally broad spectral sensitivity in the eye of a butterfly, *Papilio xuthus*. J Neurosci 23:4527-4532

Arikawa K, Pirih P, Stavenga DG (2009) Rhabdom constriction enhances filtering by the red screening pigment in the eye of the Eastern Pale Clouded yellow butterfly, *Colias erate* (Pieridae). J Exp Biol 212:2057-2064

Arikawa K, Scholten DGW, Kinoshita M, Stavenga DG (1999) Tuning of photoreceptor spectral sensitivities by red and yellow pigments in the butterfly *Papilio xuthus*. Zool Sci 16:17-24

Arikawa K, Stavenga DG (1997) Random array of colour filters in the eyes of butterflies. J Exp Biol 200:2501-2506

Arikawa K, Wakakuwa M, Qiu X, Kurasawa M, Stavenga DG (2005) Sexual dimorphism of short-wavelength photoreceptors in the Small White butterfly, *Pieris rapae crucivora*. J Neurosci 25:5935-5942

Awata H, Matsushita A, Wakakuwa M, Arikawa K (2010) Eyes with basic dorsal and specific ventral regions in the glacial Apollo, Parnassius glacialis (Papilionidae). J Exp Biol 213:4023-4029

Awata H, Wakakuwa M, Arikawa K (2009) Evolution of color vision in pierid butterflies: blue opsin duplication, ommatidial heterogeneity and eye regionalization in *Colias erate*. J Comp Physiol A 195:401-408

Bernard GD, Miller WH (1970) What does antenna engineering have to do with insect eyes? IEEE Student J 8:2-8

Bernard GD, Remington CL (1991) Color vision in *Lycaena* butterflies: Spectral tuning of receptor arrays in relation to behavioral ecology. Proc Natl Acad Sci USA 88:2783-2787

Bernhard CG, Miller WH, Møller AR (1965) The insect corneal nipple array. Acta Phsiol Scand 63 (Suppl 243):1-79

Braby MF (2006) Molecular phylogenty and systematics of the Pieridae (Lepidoptera: Papilionoidea): higher classification and biogeography. Zool J Linne Soc 147:239-275

Briscoe AD (2000) Six opsins from the butterfly *Papilio glaucus*: Molecular phylogenetic evidence for paralogous origins of red-sensitive visual pigments in insects. J Mol Evol 51:110-121

Briscoe AD, Bybee SM, Bernard GD, Yuan F, Sison-Mangus MP, Reed RD, Warren AD, Llorente-Bousquets J, Chiao CC (2010) Positive selection of a duplicated UV-sensitive visual pigment coincides with wing pigment evolution in Heliconius butterflies. Proc Natl Acad Sci USA 107:3628-3633

Cheng CL, Novales Flamarique I (2004) Opsin expression: New mechanism for modulating colour vision. Nature 428:279-279

Frentiu FD, Bernard GD, Cuevas CI, Sison-Mangus MP, Prudic KL, Briscoe AD (2007a) Adaptive evolution of color vision as seen through the eyes of butterflies. Proc Natl Acad Sci USA 104:8634-8640

Frentiu FD, Bernard GD, Sison-Mangus MP, Brower AV, Briscoe AD (2007b) Gene duplication is an evolutionary mechanism for expanding spectral diversity in the long-wavelength photopigments of butterflies. Mol Biol Evol 24:2016-2028

Frisch Kv (1914) Der Farbensinn und Formensinn der Biene. Zool J Physiol 37:1-238

Gordon WC (1977) Microvillar orientation in the retina of the nymphalid butterfly. Z Naturforsch 32c:662-664

Govardovskii VI, Fyhrquist N, Reuter T, Kuzmin DG, Donner K (2000) In search of the visual pigment template. Visual Neurosci 17:509-528

Guindon S, Lethiec F, Duroux P, Gascuel O (2005) PHYML Online--a web server for fast maximum likelihood-based phylogenetic inference. Nucleic Acids Research 33:W557-559

Horvath G, Varju D (2004) Polarized light in animal vision: Polarization patterns in nature. Springer

Jackowska M, Bao R, Liu Z, McDonald EC, Cook TA, Friedrich M (2007) Genomic and gene regulatory signatures of cryptozoic adaptation: Loss of blue sensitive photoreceptors through expansion of long wavelength-opsin expression in the red flour beetle *Tribolium castaneum*. Front Zool 4:24

Kelber A (1999a) Ovipositing butterflies use a red receptor to see green. J Exp Biol 202:2619-2630

Kelber A (1999b) Why 'false' colours are seen by butterflies. Nature 402:251

Kelber A, Pfaff M (1999) True colour vision in the orchard butterfly, *Papilio aegeus*. Naturwissenschaften 86:221-224

Kelber A, Vorobyev M, Osorio D (2003) Animal colour vision--behavioural tests and physiological concepts. Biol Rev Camb Philos Soc 78:81-118

Kinoshita M, Arikawa K (2000) Colour constancy of the swallowtail butterfly, *Papilio xuthus*. J Exp Biol 203:3521-3530

Kinoshita M, Shimada N, Arikawa K (1999) Colour vision of the foraging swallowtail butterfly *Papilio xuthus*. J Exp Biol 202:95-102

Kinoshita M, Takahashi Y, Arikawa K (2008) Simultaneous color contrast in the foraging swallowtail butterfly, *Papilio xuthus*. J Exp Biol 211:3504-3511

Kitamoto J, Sakamoto K, Ozaki K, Mishina Y, Arikawa K (1998) Two visual pigments in a single photoreceptor cell: Identification and histological localization of three mRNAs encoding visual pigment opsins in the retina of the butterfly *Papilio xuthus*. J Exp Biol 201:1255-1261

Kolb G (1978) Zur Rhabdomstruktur des Auges von *Pieris brassicae* L. (Insecta, Lepidoptera). Zoomorphologie 91:191-200

Kolb G (1986) Retinal ultrastructure in the dorsal rim and large dorsal area of the eye of *Aglais urticae* (Lepidoptera). Zoomorphology 106:244-246

Koshitaka H, Kinoshita M, Vorobyev M, Arikawa K (2008) Tetrachromacy in a butterfly that has eight varieties of spectral receptors. Proc Biol Sci 275:947-954

Labhart T, Baumann F, Bernard GD (2009) Specialized ommatidia of the polarization-sensitive dorsal rim area in the eye of monarch butterflies have non-functional reflecting tapeta. Cell Tissue Res

Loew ER, Govardovskii VI, Röhlich P, Szél A (1996) Microspectrophotometric and immunocytochemical identification of ultraviolet photoreceptors in geckos. Visual Neurosci 13:247-256

Makino CL, Dodd RL (1996) Multiple visual pigments in a photoreceptor of the salamander retina. J Gen Physiol 108:27-34

Mazzoni EO, Celik A, Wernet MF, Vasiliauskas D, Johnston RJ, Cook TA, Pichaud F, Desplan C (2008) Iroquois complex genes induce co-expression of rhodopsins in *Drosophila*. PLoS Biology 6:e97

Menzel R (1979) Spectral sensitivity and color vision in invertebrates. In: Autrum H (ed) Handbook of Sensory Physiology. Springer-Verlag, Berlin Heidelberg New York, pp 503-580

Menzel R, Backhaus W (1989) Color vision in honey bees: Phenomena and physiological mechanisms. Stavenga DG, Hardie RC (eds) Facets of vision. Springer-Verlag, Berlin Heidelberg New York London Paris Tokyo, pp 281-297

Nakanishi Y, Watanabe M, Ito T (2000) Differences in lifetime reproductive output and mating frequency of two female morphs of the sulfur butterfly, Colias erate (Lepidoptera: Pieridae). J Res Lepidoptera 35:1–8

Ogawa Y, Awata H, Wakakuwa M, Kinoshita M, Stavenga DG, Arikawa K (2012) Coexpression of three middle wavelength-absorbing visual pigments in sexually dimorphic photoreceptors of the butterfly *Colias erate*. J Comp Physiol A 198:857-867

Pichaud F, Briscoe A, Desplan C (1999) Evolution of color vision. Curr Opin Neurobiol 9:622-627

Pirih P, Arikawa K, Stavenga DG (2010) An expanded set of photoreceptors in the Eastern Pale Clouded Yellow butterfly, *Colias erate*. J Comp Physiol A 196:501-517

Qiu X, Arikawa K (2003a) The photoreceptor localization confirms the spectral heterogeneity of ommatidia in the male small white butterfly, *Pieris rapae crucivora*. J Comp Physiol A 189:81-88

Qiu X, Arikawa K (2003b) Polymorphism of red receptors: Sensitivity spectra of proximal photoreceptors in the small white butterfly, *Pieris rapae crucivora*. J Exp Biol 206:2787-2793

Qiu X, Vanhoutte KA, Stavenga DG, Arikawa K (2002) Ommatidial heterogeneity in the compound eye of the male small white butterfly, *Pieris rapae crucivora*. Cell and Tissue Research 307:371-379

Rajkumar P, Rollmann SM, Cook TA, Layne JE (2010) Molecular evidence for color discrimination in the Atlantic sand fiddler crab, *Uca pugilator*. J Exp Biol 213:4240-4248

Ribi WA (1979) Coloured screening pigments cause red eye glow hue in Pierid butterflies. J Comp Physiol A 132:1-9

Roehlich P, Vanveen T, Szel A (1994) Two different visual pigments in one retinal cone cell. Neuron 13:1159-1166

Schaefer MH, Schaefer V, Vorobyev M (2007) Are fruit colors adapted to consumer vision and birds equally efficient in detecting colorful signals? American Naturalist 169:S159-S169

Sison-Mangus MP, Bernard GD, Lampel J, Briscoe AD (2006) Beauty in the eye of the beholder: the two blue opsins of lycaenid butterflies and the opsin gene-driven evolution of sexually dimorphic eyes. J Exp Biol 209:3079-3090

Stavenga DG (1979) Pseudopupils of compound eyes. In: Autrum H (ed) Handbook of Sensory Physiology. Springer-Verlag, Berlin Heidelberg New York, pp 357-439

Stavenga DG (1989) Pigments in compound eyes. In: Stavenga DG, Hardie RC (eds) Facets of vision. Springer-Verlag, Berlin Heidelberg New York London Paris Tokyo, pp 152-172

Stavenga DG (2002) Reflections on colourful ommatidia of butterfly eyes. J Exp Biol 205:1077-1085

Stavenga DG, Arikawa K (2008) One rhodopsin per photoreceptor: *Iro-C* genes break the rule. PLoS

Biology 6:115

Stavenga DG, Arikawa K (2011) Photoreceptor spectral sensitivities of the Small White butterfly *Pieris rapae crucivora* interpreted with optical modeling. J Comp Physiol A 197:373-385

Stavenga DG, Kinoshita M, Yang EC, Arikawa K (2001) Retinal regionalization and heterogeneity of butterfly eyes. Naturwissenschaften 88:477-481

Takemura SY, Arikawa K (2006) Ommatidial type-specific interphotoreceptor connections in the lamina of the swallowtail butterfly, *Papilio xuthus*. Journal of Comparative Neurology 494:663-672

Takemura SY, Stavenga DG, Arikawa K (2007) Absence of eye shine and tapetum in the heterogeneous eye of *Anthocharis* butterflies (Pieridae). J Exp Biol 210:3075-3081

Tamura K, Dudley J, Nei M, Kumar S (2007) MEGA4: Molecular Evolutionary Genetics Analysis (MEGA) software version 4.0. Mol Biol Evol 24:1596-1599

von Helversen O (1972) Zur spektralen Unterschiedsempfindlichkeit der Honigbiene. J Comp Physiol A 80:439-472

Vorobyev M (2003) Coloured oil droplets enhance colour discrimination. Proc Biol Sci 270:1255-1261

Vorobyev M, Osorio D (1998) Receptor noise as a determinant of colour thresholds. Proc Biol Sci 265:351-358

Wakakuwa M, Kurasawa M, Giurfa M, Arikawa K (2005) Spectral heterogeneity of honeybee ommatidia. Naturwissenschaften 92:464-467

Wakakuwa M, Stavenga DG, Arikawa K (2006) Spectral organization of ommatidia in flower-visiting insects. Photochem Photobiol 83:27-34

Wakakuwa M, Stavenga DG, Kurasawa M, Arikawa K (2004) A unique visual pigment expressed in green, red and deep-red receptors in the eye of the Small White butterfly, *Pieris rapae crucivora*. J Exp Biol 207:2803-2810

Wakakuwa M, Terakita A, Koyanagi M, Stavenga DG, Shichida Y, Arikawa K (2010) Evolution and mechanism of spectral tuning of blue-absorbing visual pigments in butterflies. PLoS ONE 5:e15015

Yagi N, Koyama N (1963) The compound eye of Lepidoptera. Approach from organic evolution. Maruzen, Tokyo

Zaccardi G, Kelber A, Sison-Mangus MP, Briscoe AD (2006) Color discrimination in the red range with only one long-wavelength sensitive opsin. J Exp Biol 209:1944-1955